

Evaluation of Wall-Modeled LES for Turbulent Separated Flows

Prahladh S. Iyer

National Institute of Aerospace, Hampton, VA

Mujeeb R. Malik

NASA Langley Research Center, Hampton, VA



NASA Ames AMS Seminar

Thursday, August 27, 2020

Motivation

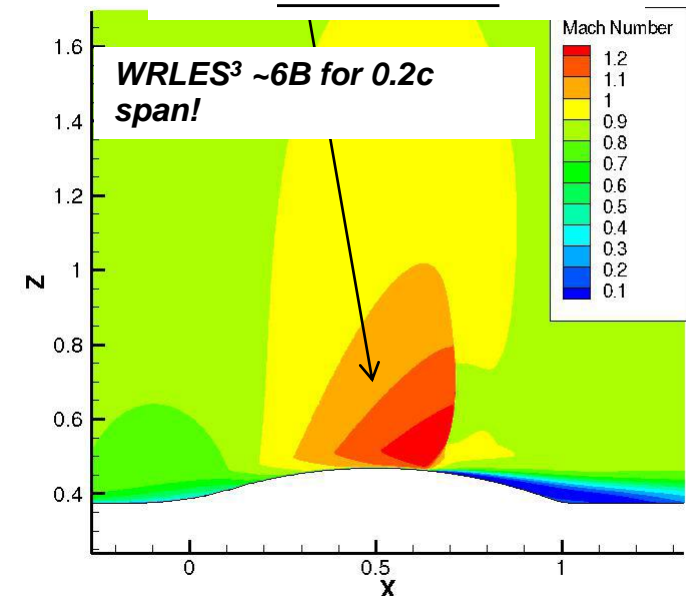
- CFD increasingly used for design in aeronautical industry. **Challenging** to accurately predict **flow separation**.

<u>RANS</u>	<u>DNS/ LES</u>
Computationally inexpensive	Excellent predictive capability for flows with separation
Poor predictive capability for flows with separation	Computationally very expensive for high Re
	DNS grid points $\sim Re_{Lx}^{37/14}$ for a flat plate of Length Lx

- Can WMLES bridge the gap by resolving large scales in outer layer and modeling near-wall inner layer ?
- Assess **benefits/ limitations** of WMLES for **turbulent separated flows** at various **Mach numbers** towards application in an aircraft configuration across full flight envelope: Grand Challenge Problem, NASA CFD Vision 2030 study.



Boeing 787 Dreamliner¹



¹ Figure taken from : https://en.wikipedia.org/wiki/Boeing_787_Dreamliner

² Uzun & Malik (AIAA 2018)

Outline of Presentation

❑ Wall Model Methodology

- ❖ Potential Sources of Error in WMLES
- ❖ Improved Damping Function Scaling for High-Speed Flows

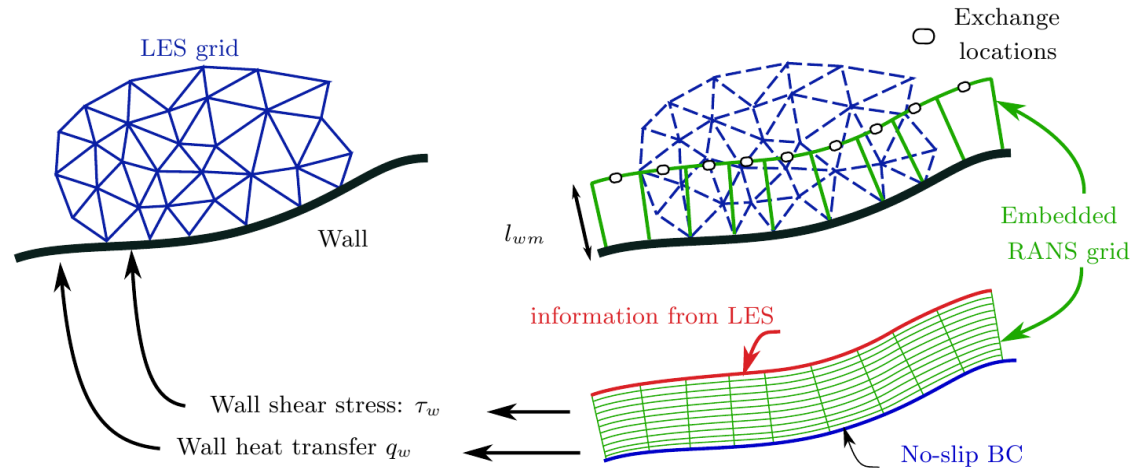
❑ Two-dimensional/ Axisymmetric RCA Test Cases

- ❖ Mach 0.1 NASA Hump
- ❖ Mach 0.875 Bachalo Johnson Bump

❑ Juncture Flow Results

❑ Summary

Equilibrium Wall Model



- Compressible equilibrium BL ODEs solved in WM region (Kawai & Larsson 2012):

$$\frac{d}{d\eta} \left[(\mu + \mu_{t,wm}) \frac{du_{\parallel}}{d\eta} \right] = 0$$

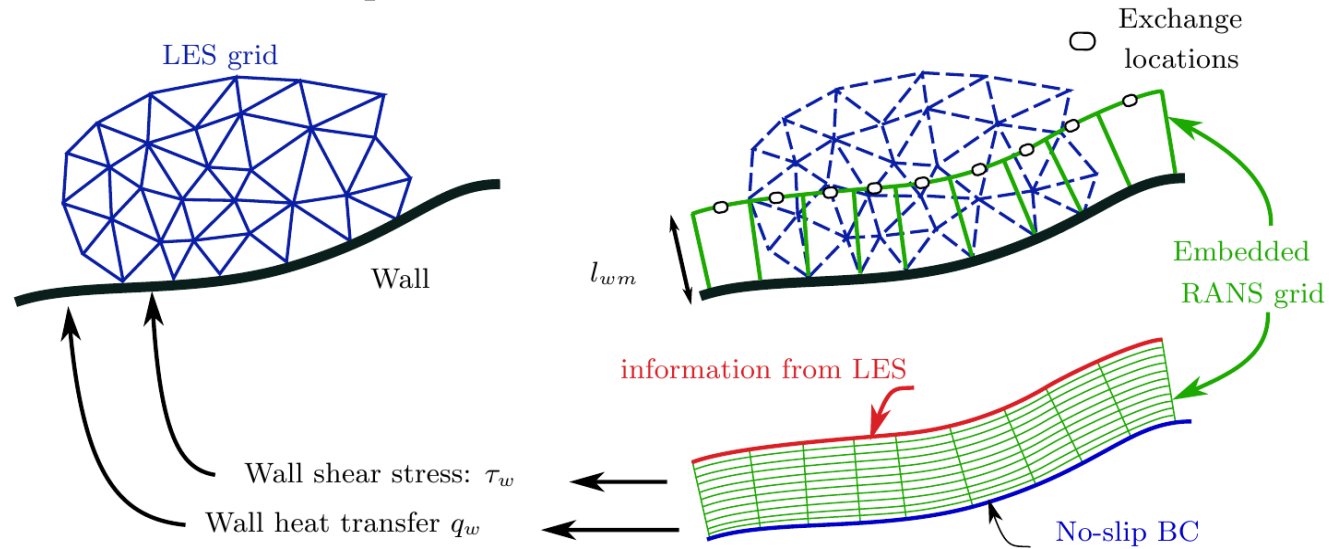
$$\frac{d}{d\eta} \left[(\mu + \mu_{t,wm}) u_{\parallel} \frac{du_{\parallel}}{d\eta} + (\lambda + \lambda_{t,wm}) \frac{dT}{d\eta} \right] = 0$$

- Eddy viscosity obtained from mixing-length model and turbulent thermal conductivity obtained assuming constant $Pr_t=0.9$.

$$\mu_{t,wm} = \kappa \eta \rho \sqrt{\frac{\tau_w}{\rho}} \left[1 - \exp\left(-\frac{\eta^+}{A^+}\right) \right]^2 \quad (A^+=17, \kappa=0.41)$$

$$\tau_i = \tau_{\parallel} \frac{u_i}{u_{\parallel}} \quad (\text{Potentially inaccurate for complex 3D flows})$$

Nonequilibrium Wall Model



- Full 3D compressible URANS equations (Park & Moin 2014):

$$\mu_{t,wm}^* = \rho(\kappa\eta)^2 |S| \left[1 - \exp\left(-\frac{\eta^+}{A^+}\right) \right]^2 \quad (A^+=26, \kappa=0.41)$$

- Total Reynolds stresses (modeled+resolved) modeled using standard values of mixing-length model.

$$2\mu_{t,wm} \bar{S}_{ij}^d - \frac{2}{3} \bar{\rho} k \delta_{ij} - \bar{\rho} \bar{R}_{ij} \approx 2\mu_{t,wm}^* \bar{S}_{ij}^d - \frac{2}{3} \bar{\rho} k^* \delta_{ij}$$

$$\mu_{t,wm} = \mu_{t,wm}^* + \frac{\bar{\rho} \bar{R}_{ij} \bar{S}_{ij}^d}{2 \bar{S}_{lm}^d \bar{S}_{lm}^d}$$

- Incorporates nonequilibrium effects such as pressure gradient, but more expensive.
- Effective κ (in $\mu_{t,wm}$) clipped so that it lies between $[0, 0.41]$.

Potential Sources of Error in WMLES

Potential Sources of Error

- **LES errors:**

1. **Grid** : resolution (Δx^+ , δ/n_{xi}), quality (skewness, stretching), anisotropy ($\Delta x/\Delta z$, $\Delta x/\Delta y$)
We use: 10-40 ppd, nearly isotropic cells with near-wall stretching
2. **Numerics + SGS Model** : Central vs. Upwind, Explicit vs. Implicit LES
We use: low-dissipation fluxes with Vreman SGS model.
3. **Grid convergence (and adaptation)** : a challenge for LES as SGS model (or numerical dissipation for ILES) a function of filter width that is implicitly set by the grid.
4. Synthetic inflow turbulence OR transition/tripping

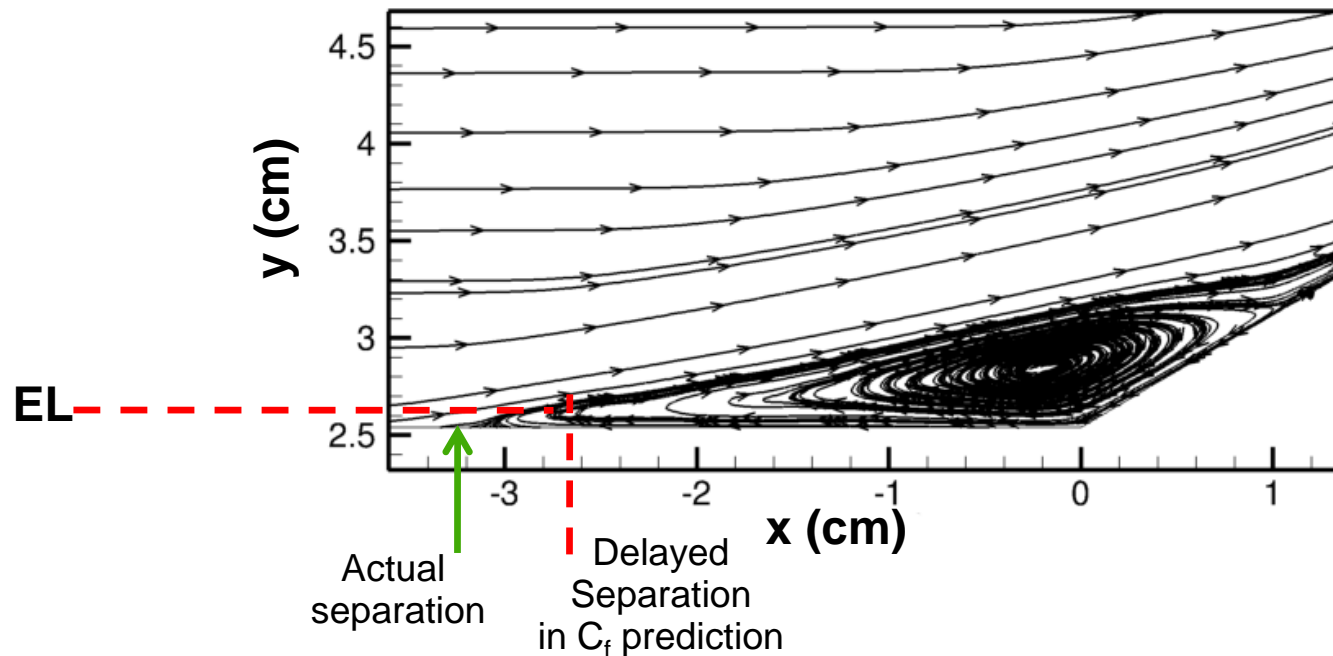
- **Wall-model errors:**

1. **Eddy-viscosity model** : κ , A^+ , compressibility effects
2. **Some challenges**: effects of dp/dx , relaminarization, strong curvature effects
3. Eddy-viscosity model tuned for time-averaged flow, but used in an instantaneous setting.

Potential Sources of Error

- WMLES errors:

1. Erroneous skin-friction a.k.a. log-layer mismatch (LLM) error:
 - a) Use EL away from the wall (Kawai & Larsson 2012)
 $\geq 2^{\text{nd}}$ wall-normal point with EL at $0.05-0.1 \delta$, and $> 1 \Delta x_{i,\text{wall}}$
 - b) Time-filtering of WM input (Yang, Park & Moin 2016)
2. Effect of EL for predicting separation location, especially for EQWM since $\vec{\tau} \parallel \vec{u}_{\text{EL}}$.
Potentially introduces some error in the NEQWM model too since the eddy viscosity model is not perfect!



3. For EQWM, the separation and reattachment locations will be different when computed based on the C_f vector, and based on **the near-wall velocity vector** if $\text{EL} > 1^{\text{st}}$ grid point.

Potential Sources of Error

- **WMLES errors (contd.):**

4. Wall shear stress fluctuations not accurately predicted (Park & Moin 2016), but wall pressure fluctuations reasonably well predicted. > 50% error for 40 ppd in turbulent channel flow.

Case	$\Delta x^+ / \Delta z^+$	$\bar{\tau}_1$	$p_{w,rms}^+$	$\tau_{1,rms}^+$	$\tau_{3,rms}^+$
Present WMLES (baseline)	200/125	1.027(1.035)	3.836(3.858)	0.226(0.197)	0.150(0.073)
Present WMLES (xz-refined-1)	100/62.5	0.998(1.001)	2.917(2.951)	0.191(0.185)	0.105(0.069)
Present WMLES (xz-refined-2)	50/31.25	(0.999)	(2.915)	(0.196)	(0.075)
Incompressible DNS [26]	8.2/4.1	1	2.817	0.431	0.289

$Re_\tau = 2000$ channel NEQWM (EQWM) results, EL at $y^+ = 200$ from Park & Moin (2016)

5. Implications for prediction of flow separation/reattachment locations, especially incipient and highly unsteady regimes.

- **EQWM vs. NEQWM for accelerating, pressure gradient regions:**

1. EQWM returns erroneous τ_w when compared to NEQWM in such regions unless EL is deep in the viscous sublayer ($y^+ < 3$).
2. *If* acceleration and/or dp/dx flux terms dominate relative to the total wall-normal stress terms in strongly nonequilibrium regions, erroneous τ_w *may* not really affect the LES solution!

Potential Sources of Error

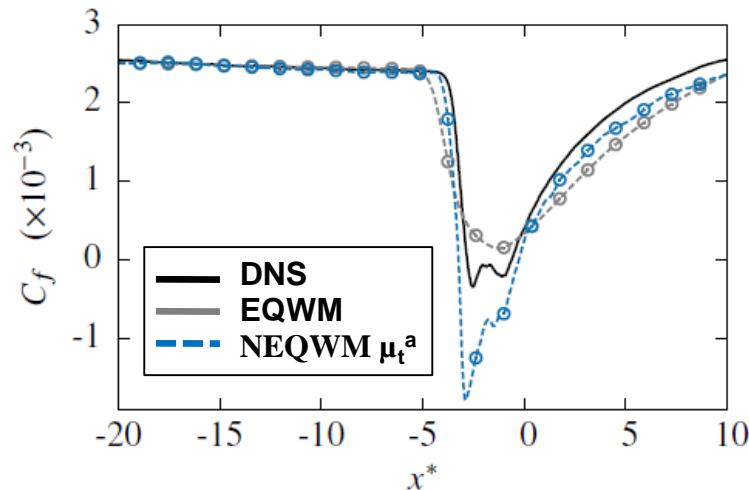
3. Replace EQWM with no-slip BC near separation and reattachment?

Since $C_f \rightarrow 0$ in these regions, EL will always lie in the viscous sublayer and so no-slip and EQWM would return the same result in the time-averaged sense. Inside the bubble, typically $|C_f| \ll |C_f|_{BL}$, and so EL^+ would be < 10 in separation region.

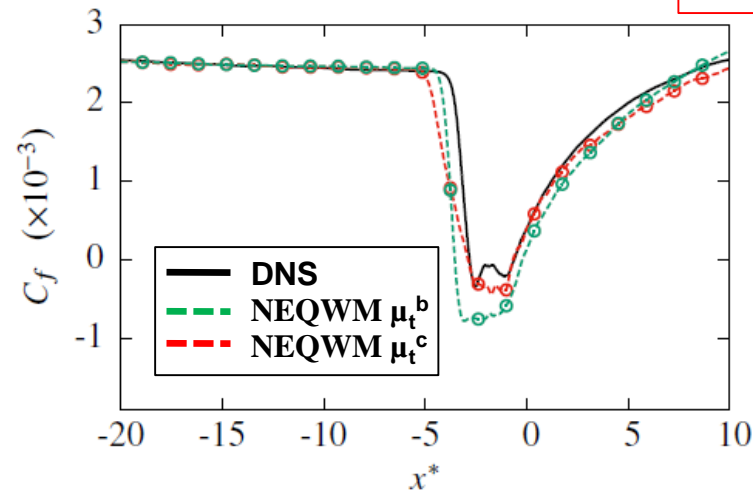
4. NEQWM not free of errors in separation/ pressure gradient regions:

Mach 2.3, Re_τ 450 oblique SWBLI data from Mettu & Subbareddy (AIAA-2019-3699)

$$\mu_t^a = \rho(\kappa y)^2 |S| D_2(y), \quad D_2(y) = (1 - \exp(-y^+ / A_2^+))^2$$



$$\mu_t^c = \rho(\kappa y)^2 |S| D_p(y)$$



$$\mu_t^b = \rho(\kappa y)^2 |S| D_p(y) \alpha_*^{-0.5} (\alpha_* + y_p (1 - \alpha_*)^{1.5})^{0.5}$$

$$D_p(y) = (1 - \exp(-y_p / A_3^+))^2, \quad A_3^+ = 1 + \alpha_*^3 (A_2^+ - 1)$$

$$u_{\tau p}^2 = u_\tau^2 + (1 - \alpha_*) u_p^2, \quad y_p = y u_{\tau p} / \nu$$

Improved Damping Function Scaling for High-Speed Flows

Iyer & Malik, *Phys. Rev. Fluids* 2019

Damping Function for Compressible Flows

$$\mu_t = \rho k y \sqrt{\frac{\tau_w}{\rho}} D_{VD}, \quad D_{VD} = \left[1 - \exp\left(-\frac{y_c^+}{A^+}\right) \right]^2 \quad (A^+ = 17)$$

Some proposals exist where A^+ or equivalent = $f(M, T_w \dots)$ but not considered here

$$y_{wall}^+ = \frac{\rho_w u_\tau y}{\mu_w}$$

Traditionally used for compressible flows,
Kawai & Larsson (2012), Larsson et al. (2016)
Works better for adiabatic flows

$$y_{SL}^+ = \frac{\sqrt{\rho_w \rho} u_\tau y}{\mu}$$

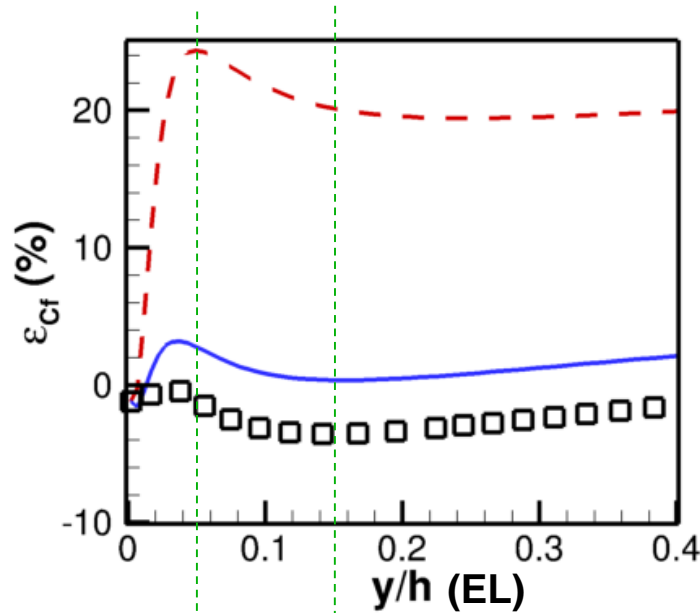
More recently recommended scaling by *Aupoix & Viala (1995), Bocquet, Sagaut & Jouhaud (2012), Yang & Lv (2018), Larsson (wmles.umd.edu)*.
Works better for cold-wall flows

$$y_{mixed \min 2}^+ = \frac{1}{2} \left[\frac{\sqrt{\rho \rho_w} u_\tau y}{\mu} + \min\left(\frac{\rho_w u_\tau y}{\mu_w}, \frac{\rho u_\tau y}{\mu}\right) \right]$$

Iyer & Malik (2019) proposed mixed scaling based on empirical observations. Works better than the previous scalings, but needs improvement for intermediate thermal conditions ($T_w/T_{ad} \sim 0.5$)

A Priori Assessment of Existing Models

$M_b=1.5$
 $Re_\tau = 1011$
 $T_w/T_{ad} \sim 0.46$
 $T_w/T_\infty \sim 0.73$
 Channel
 Modesti &
 Pirozzoli (2016)



Typical exchange location in WMLES

$$\mu_t = \rho \kappa y \sqrt{\frac{\tau_w}{\rho}} \left[1 - \exp\left(-\frac{y_c^+}{17}\right) \right]^2$$

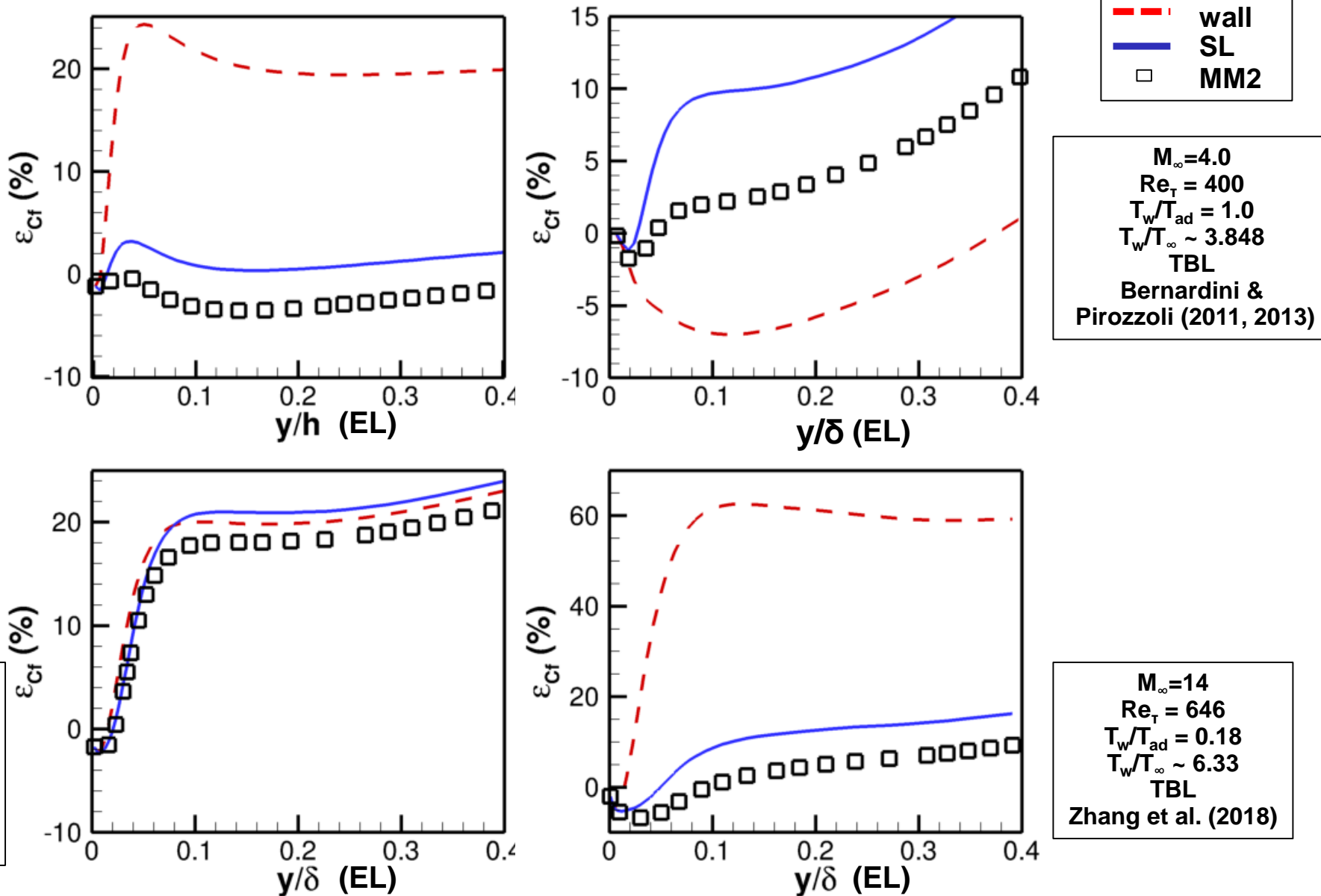
Abscissa (x-axis) : Exchange location (EL) at which DNS data was input to the wall model

Ordinate (y-axis) : Error in C_f prediction if the corresponding y/h (or y/δ for TBL) location was used as the exchange location.

$$\varepsilon_{C_f} (\%) = \left(\frac{C_{f,wm} - C_{f,DNS}}{C_{f,DNS}} \right) \times 100$$

- Typical exchange locations used in WMLES: 0.05 – 0.15 y/h (or y/δ for TBL)

A Priori Assessment of Existing Models



- Here, y/h or y/δ is the exchange location at which DNS data was input to the wall model
- Mixedmin2 model works well in $0.05-0.15\delta$ except for $T_w/T_{ad} = 0.48$, Mach 8 TBL

A *Priori* Assessment of Existing Models

TABLE I. Errors in prediction of wall quantities (Q) at an exchange location (y/h or y/δ) of 0.05 or 0.1 are listed using the JK mixing-length model. The errors are highlighted in red, blue, and green for error magnitudes greater than 10%, 5–10%, and less than or equal to 5%, respectively.

Case	M	Re_τ	$\frac{T_w}{T_{ad}}$	Q	Wall	SL	Local	SA	mixedmin	mixedmin2
Ref. [26]	1.5	222	0.46	C_f	7.9, 26.2	2.5, 8.6	0.6, 2.5	-4.3, 1.3	2.5, 8.6	1.5, 5.6
				B_q	2.6, 12.9	0.4, 5.2	-0.3, 2.5	-2.2, 2.4	0.4, 5.2	0.1, 3.8
	3.0	451	0.18	C_f	39.2, 83.2	3.9, 10.2	-3.9, -8.6	-4.8, 2.4	3.9, 10.2	0.1, 1.1
				B_q	14.2, 34.4	0.1, 5.6	-3.1, -3.3	-3.4, 2.4	0.1, 5.6	-1.6, 1.2
Ref. [29]	1.5	1011	0.46	C_f	24.4, 21.7	2.7, 0.9	-5.2, -7.4	1.9, 1.2	2.7, 0.9	-1.0, -3.0
				B_q	12.6, 12.0	2.7, 2.3	-1.2, -1.8	3.1, 3.3	2.7, 2.3	0.9, 0.4
Refs. [38–41]	2.0	1113	1.0	C_f	-3.2, -2.9	3.2, 3.3	5.7, 5.2	4.5, 4.4	0.2, 0.3	0.2, 0.3
				T_w	-1.7, -1.8	-1.7, -1.8	-1.7, -1.8	-1.9, -1.9	-1.7, -1.8	-1.7, -1.8
	3.0	502	1.0	C_f	-4.7, -5.8	5.8, 7.1	9.9, 11.7	5.7, 8.4	0.7, 1.1	0.7, 1.1
				T_w	-3.4, -3.5	-3.4, -3.5	-3.4, -3.5	-3.6, -3.7	-3.4, -3.5	-3.4, -3.5
	4.0	398	1.0	C_f	-5.3, -6.9	6.3, 9.7	11.0, 15.7	5.2, 11.0	0.6, 2.1	0.6, 2.1
				T_w	-4.0, -4.1	-4.0, -4.0	-4.0, -4.0	-4.2, -4.3	-4.0, -4.1	-4.0, -4.1
Ref. [28]	2.5	510	1.0	C_f	-2.2, -2.6	5.8, 7.2	9.2, 11.1	5.5, 8.6	1.9, 2.5	1.9, 2.5
				T_w	-3.0, -4.4	-3.0, -4.4	-3.0, -4.4	-3.0, -4.4	-3.0, -4.4	-3.0, -4.4
	5.86	450	0.25	C_f	33.3, 59.5	2.3, 9.5	-4.2, -3.1	-5.8, 6.7	2.3, 9.5	-1.0, 3.2
				B_q	6.8, 18.9	-6.2, -1.1	-9.1, -7.0	-9.7, -2.3	-6.2, -1.2	-7.6, -4.1
	5.86	453	0.76	C_f	2.7, 1.3	14.0, 17.1	18.6, 22.5	13.6, 18.3	8.5, 10.1	8.5, 10.1
				B_q	-14.0, -12.9	-8.9, -6.5	-7.0, -4.4	-10.6, -7.5	-11.3, -9.4	-11.3, -9.4
	7.86	480	0.48	C_f	16.2, 20.1	13.7, 20.7	13.0, 21.0	11.9, 21.6	12.9, 18.6	12.3, 17.7
				B_q	-1.7, 2.0	-2.9, 2.4	-3.2, 2.1	-3.9, 2.1	-3.2, 1.2	-3.6, 0.1
	13.86	646	0.18	C_f	43.2, 61.5	0.2, 8.6	-11.1, -8.0	-6.1, 7.8	0.2, 8.6	-5.0, 0.3
				B_q	9.3, 18.2	-8.4, -2.6	-13.7, -10.4	-11.1, -2.9	-8.4, -2.6	-11.0, -6.5

- Table from Iyer & Malik (*Phys. Rev. Fluids*, 2019)
- *A posteriori* WMLES for cold wall channel, and supersonic TBL were consistent with the trends from the *a priori* analysis.

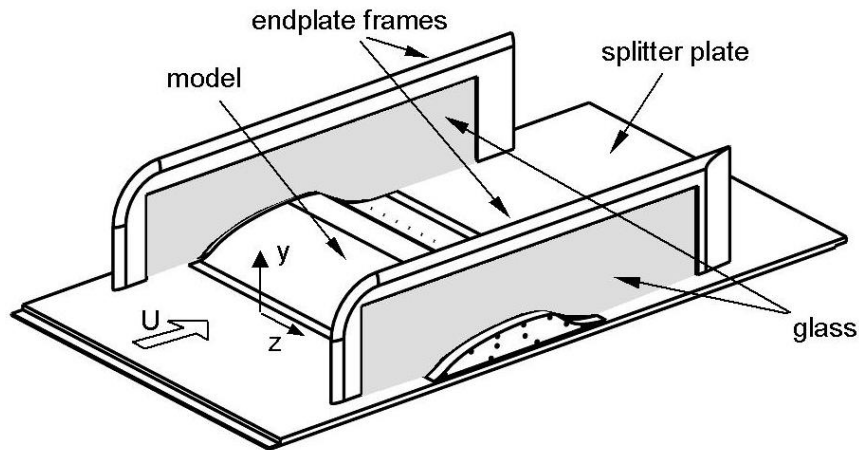
Two-dimensional/ Axisymmetric RCA Test Cases

Solver Details

- **CharLES** solver from Cascade Technologies
- **Compressible** N-S, **unstructured** finite volume discretization, **spatially 2nd order** accurate, **low numerical dissipation** solver
- **Explicit RK3** time integration
- **ENO** reconstruction + **HLLC** flux for shock-capturing with Ducros sensor
- **Const. Coeff. Vreman** SGS model
- **Synthetic Inflow** Turbulence using spatiotemporal modes method of [Shur et al.¹](#)

¹ Shur, M. L., Spalart, P. R., Strelets, M. K., & Travin, A. K. (2014). Synthetic turbulence generators for RANS-LES interfaces in zonal simulations of aerodynamic and aeroacoustic problems. *Flow, turbulence and combustion*, 93(1), 63-92.

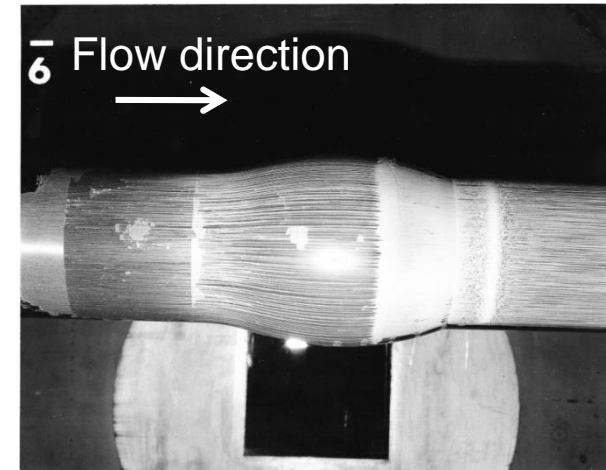
Experiment Details



Greenblatt et al. (*AIAA J.* 2006)

$M=0.1$, $Re_c = 0.936$ million

$Re_\theta \sim 7200$ (at $x/c=-2.14$)



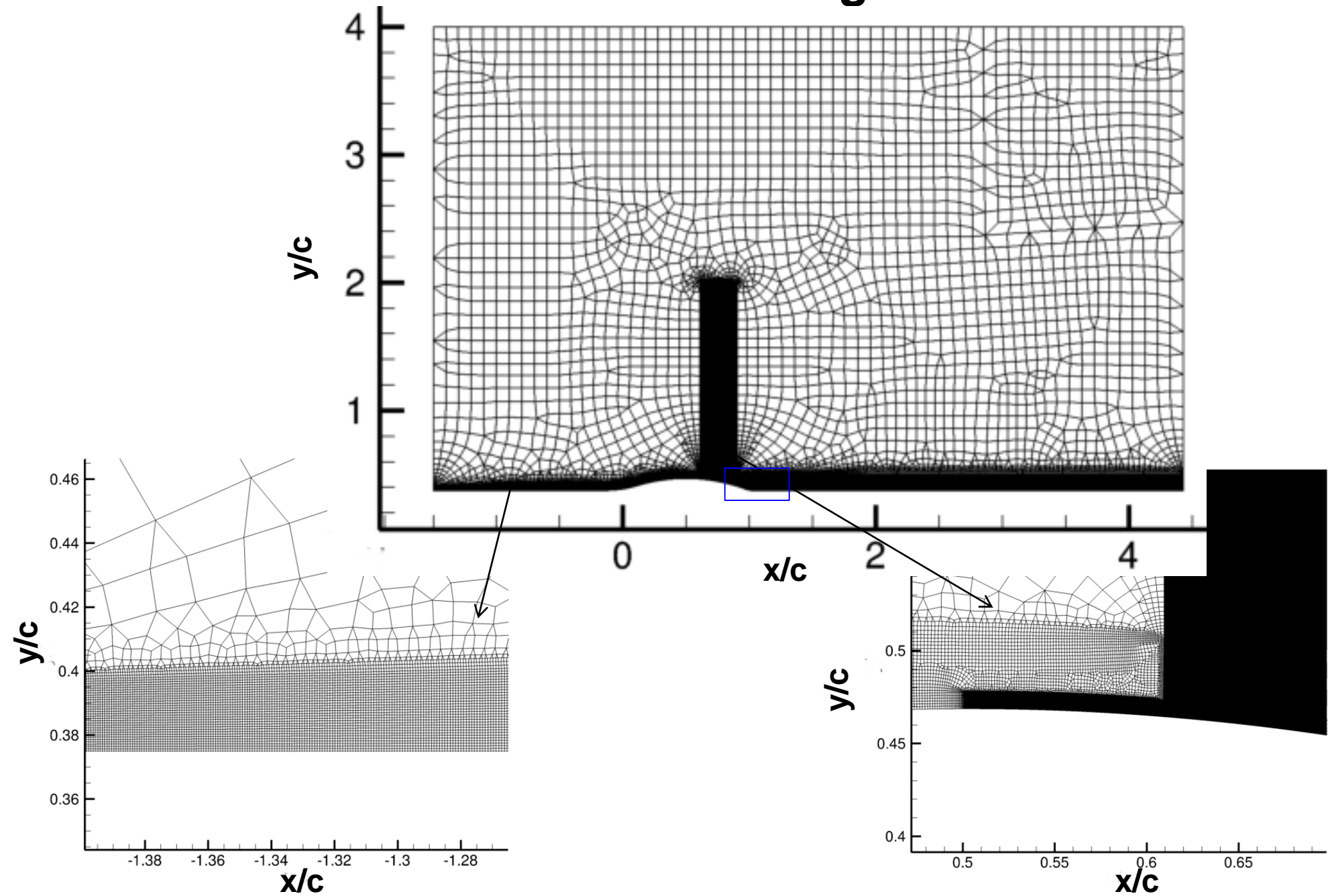
Bachalo & Johnson (*AIAA J.* 1986)

$M=0.875$, $Re_c = 2.763$ million

$Re_\theta \sim 12000$ (at $x/c=-1$)

- Tunnel wall effects not modeled for all cases. Periodic boundary conditions in the span.
- Square tunnel for axisymmetric BJ bump.
- WRLES/DNS data of Uzun & Malik (2017, 2018) available for comparison.
- Separation bubble 27% larger in the larger 6X6 ft, compared to the 2X2 ft tunnel cross-section.

Grid Design

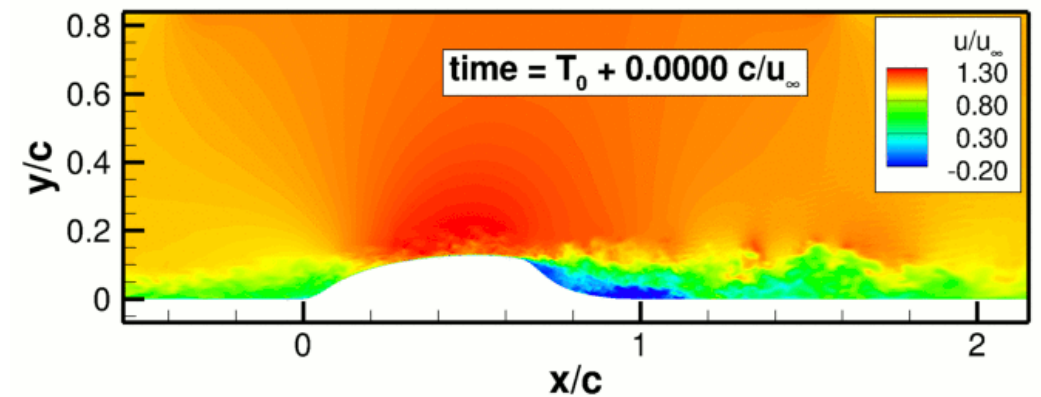
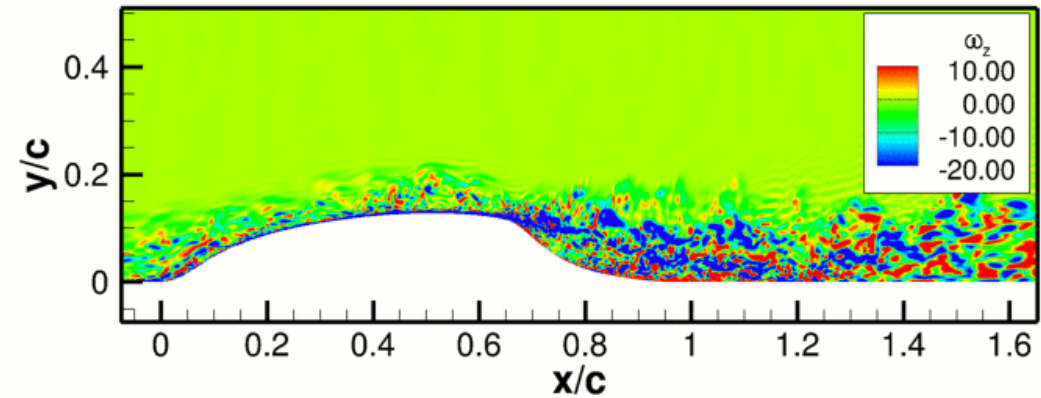
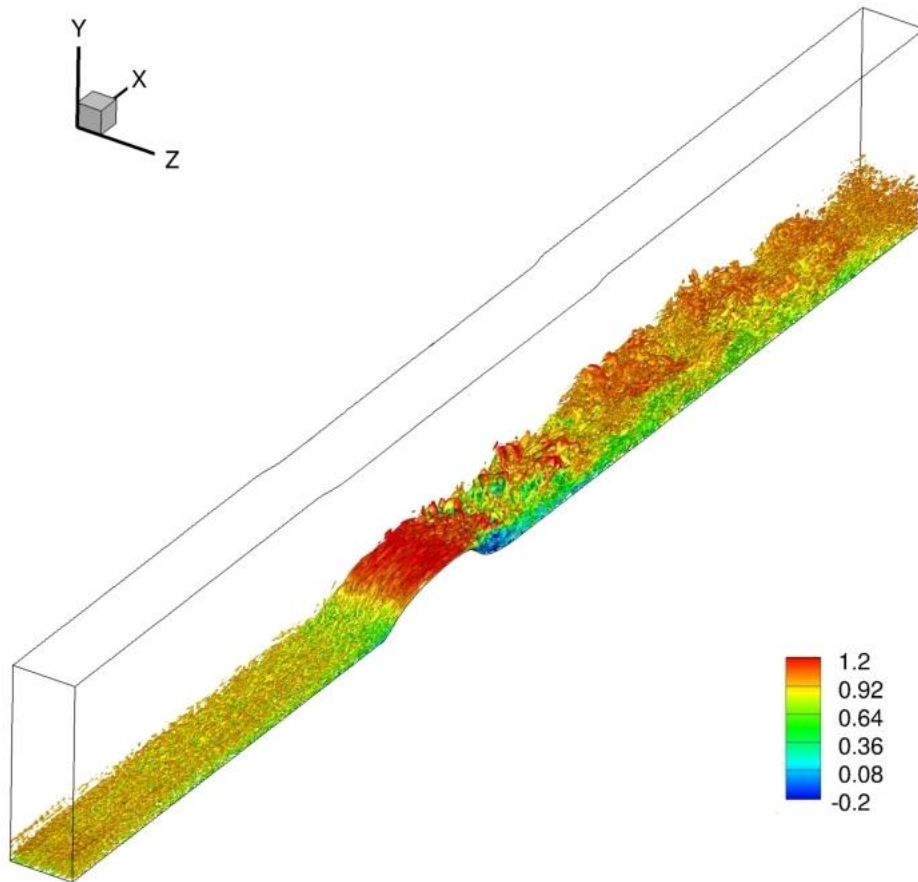


Grid Spacings

Flow	x/c	$\Delta x/c, \Delta y_{min}/c, \Delta z/c$	$\Delta x^+, \Delta y_{min}^+, \Delta z^+$	δ/c	$n_x/\delta, n_{y,min}/\delta, n_z/\delta$
NASA	-1	0.01, 1×10^{-3} , 0.005	360,36,180	0.1	10, 32, (20)
Hump	0.5	0.0015, 2×10^{-4} , 0.005	77, 10, 260	0.07	46, 32, (14)
	0.9	0.01, 3.3×10^{-3} , 0.005	300,100,150	0.2	20, 32, 40
Transonic Bump	-1.5	6.5×10^{-4} , 6.5×10^{-4} , 9.8×10^{-4}	63,63, 95	0.02	31, 31, (20)
	-0.5	1.45×10^{-3} , 1.45×10^{-3} , 9.8×10^{-4}	136, 136, 92	0.05	35, 35, 51
	0.4	1.2×10^{-3} , 1.45×10^{-3} , 9.8×10^{-4}	150, 180, 122	0.04	33, 28, 41

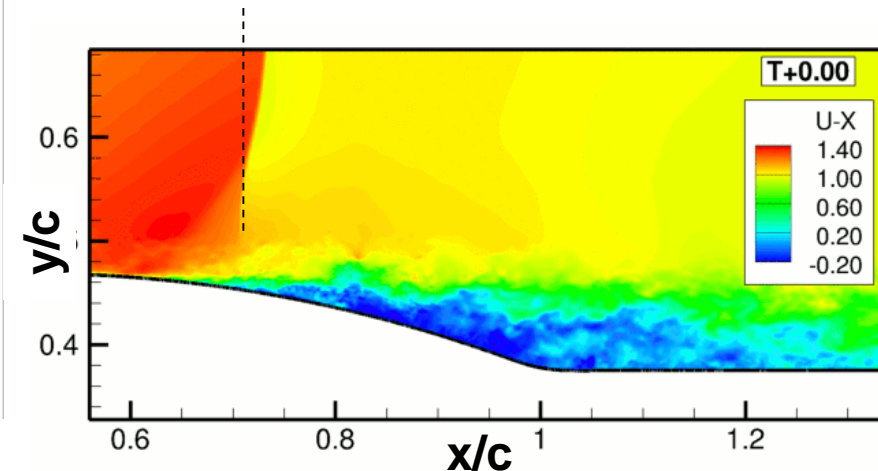
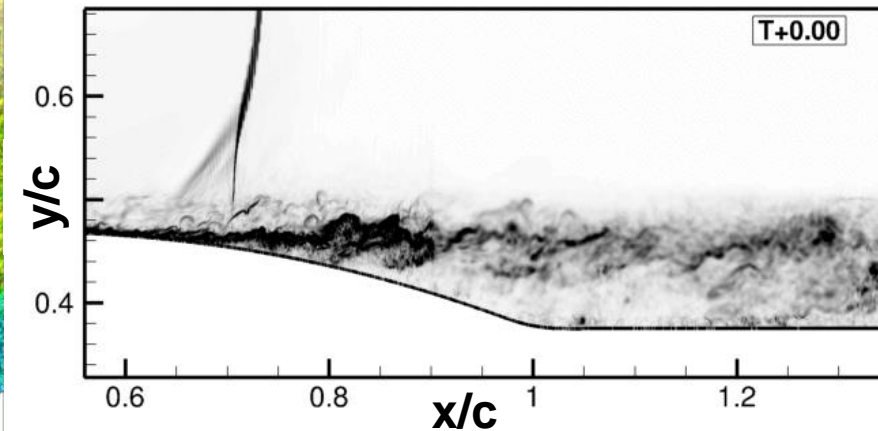
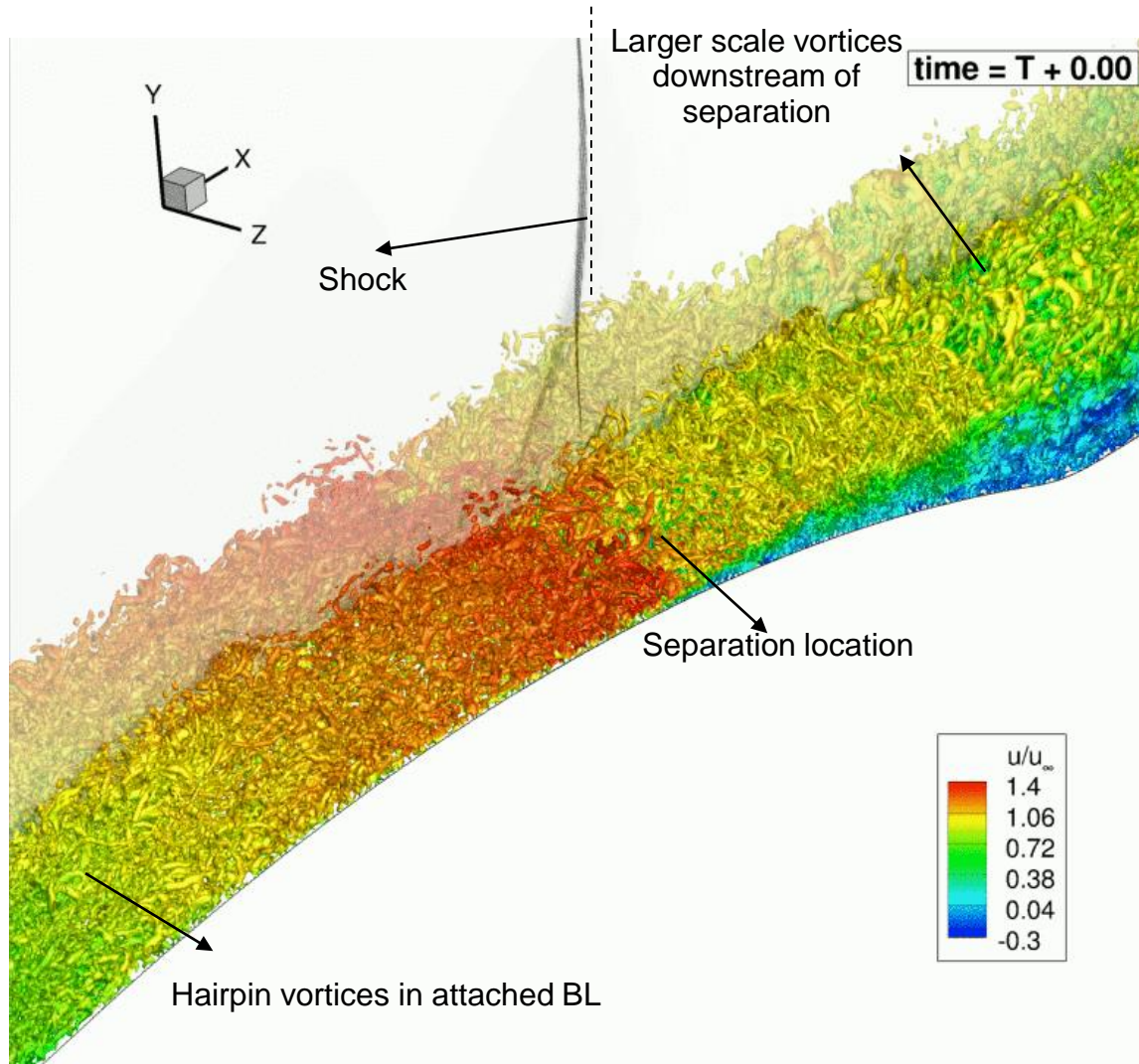
- Coarse, medium and fine grids used with grid spacings reported for medium grid.
NASA hump : 2, 10 and 37M grids, 0.3c span.
Transonic Bump : 9, 56 and (74) M grids, 30° (15 °) span.
- Coarse grid: approximately 2X coarser in each direction.
- Fine grid: has 2X refinement in spanwise spacing, and 2X refinement in x,y in the separation bubble region.
- Transonic bump medium and fine grids have ~ same Δx as DNS of Spalart et al. in the shock region.
- EL placed at ~ 5% upstream δ :
NASA hump : 0.0042 for hump [150-200 in viscous units]
Transonic bump : 0.0025 for transonic bump [> 250 in viscous units].

NASA Wall-mounted Hump



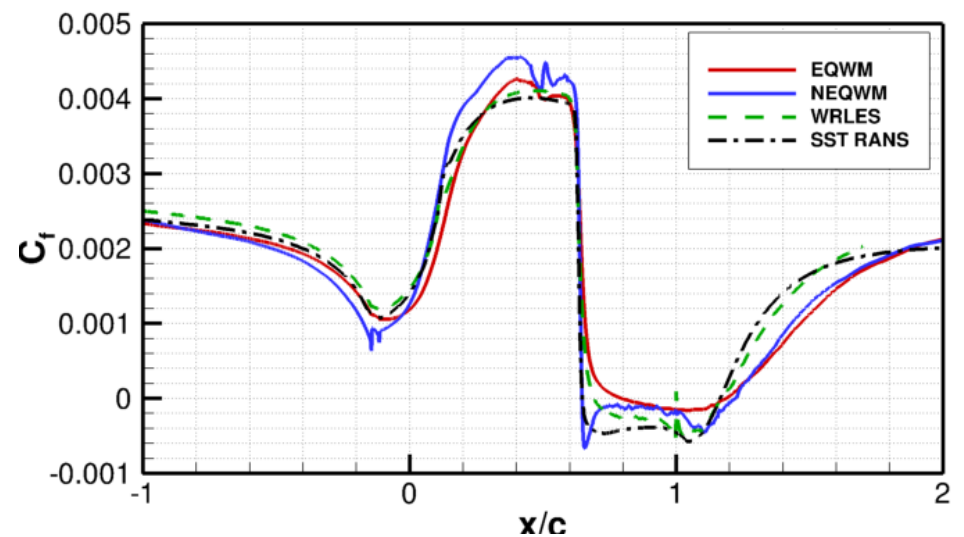
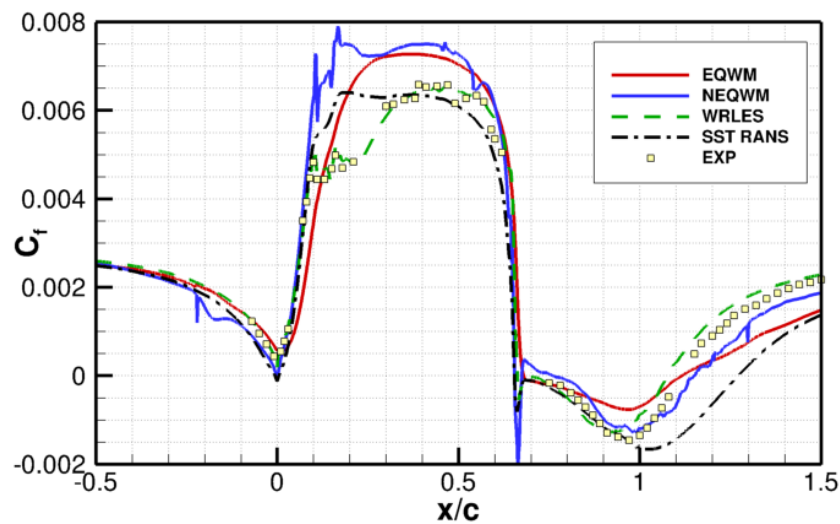
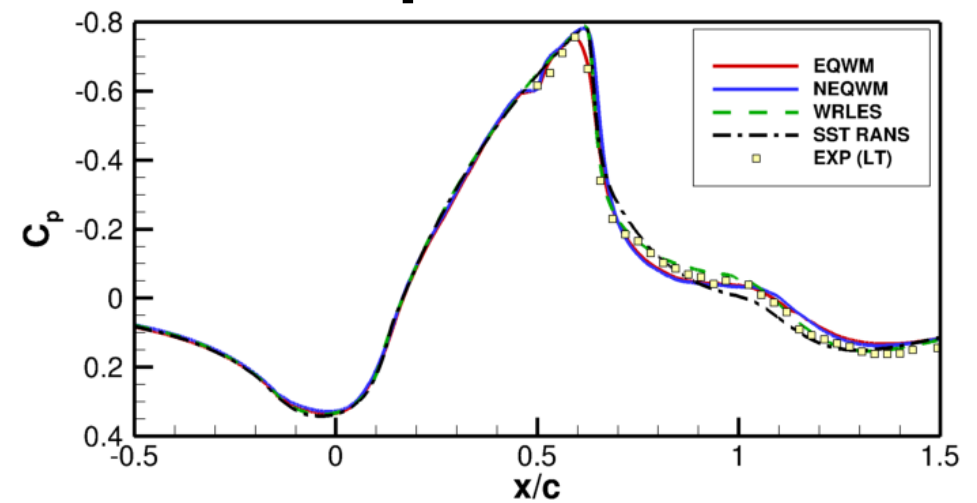
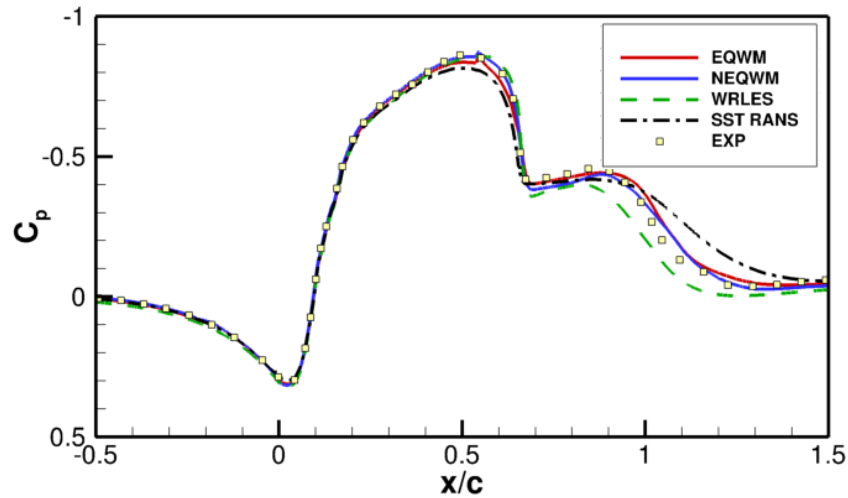
- Results from the medium 10M grid showing the unsteady features of the flow.
- More quantitative results for this grid in [Iyer & Malik AIAA-2016-3186](#).
- Experimental separation and reattachment at $x/c \sim 0.665$ and 1.105 using oil-film interferometry.

Axisymmetric Transonic Bump



- Results from the medium 56M grid showing the unsteady features of the flow.
- More quantitative results for this grid in [Iyer, Park & Malik, AIAA-2017-3953](#).
- Experimental separation and reattachment at $x/c \sim 0.675$ and 1.165 using surface oil smear technique.

Wall Pressure and Skin-friction Comparisons

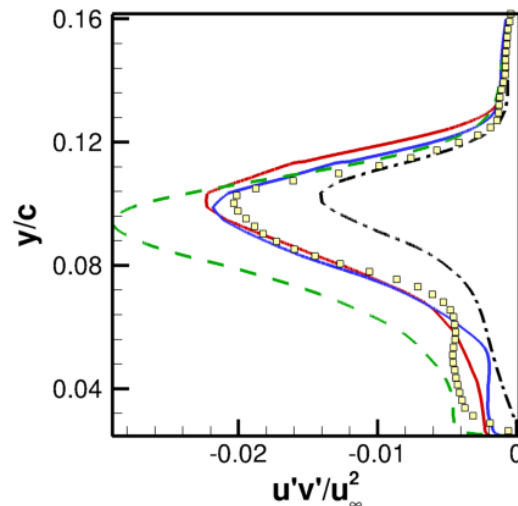
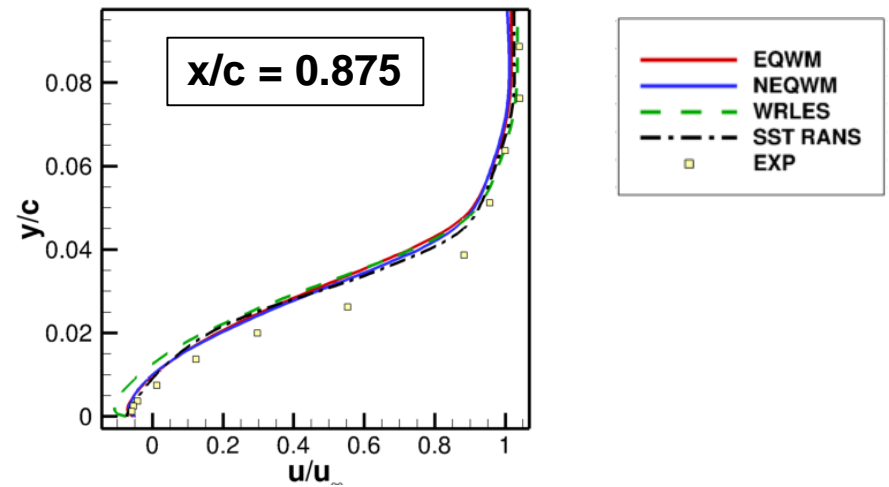
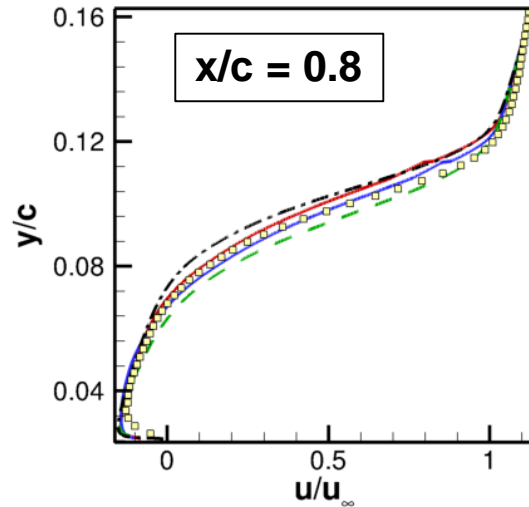


NASA Hump Fine Grid

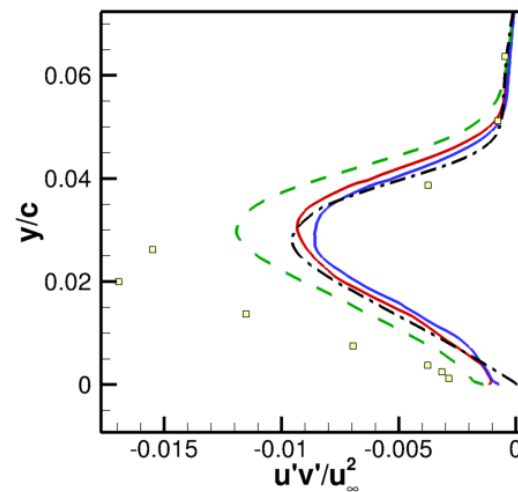
Transonic Bump Fine Grid

- Similar C_p predictions between EQWM and NEQWM. Shock location correctly predicted for the transonic case.
- Erroneous C_f for EQWM in the bubble region, and strong favorable pressure gradient region. Both models miss tendency to relaminarize for hump case.

Separation Region Comparisons



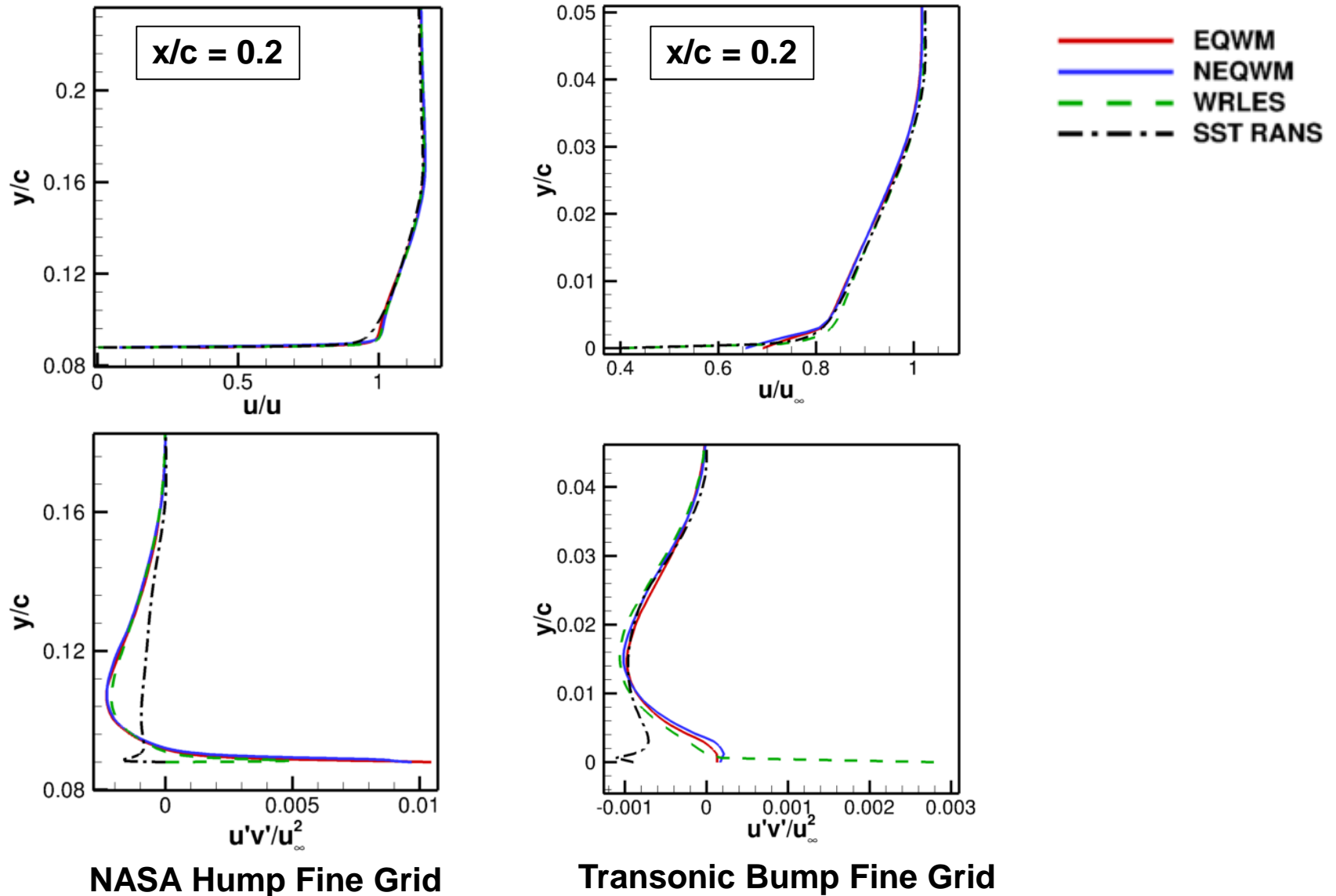
NASA Hump Fine Grid



Transonic Bump Fine Grid

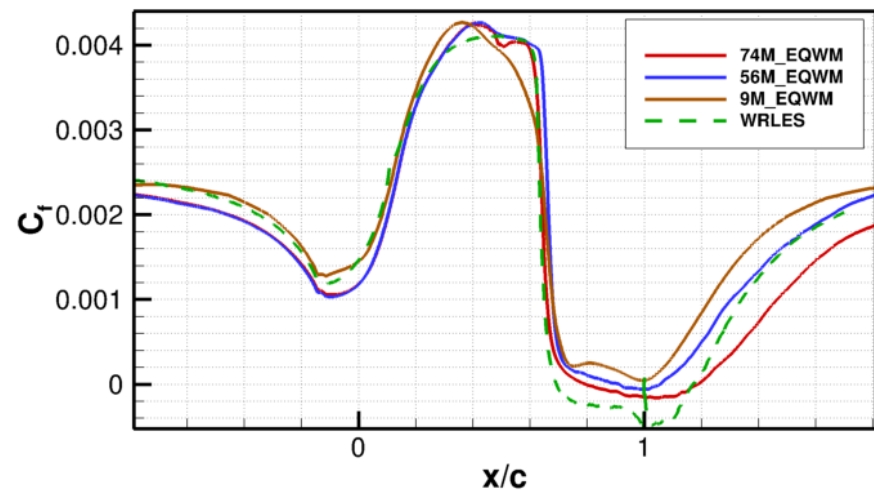
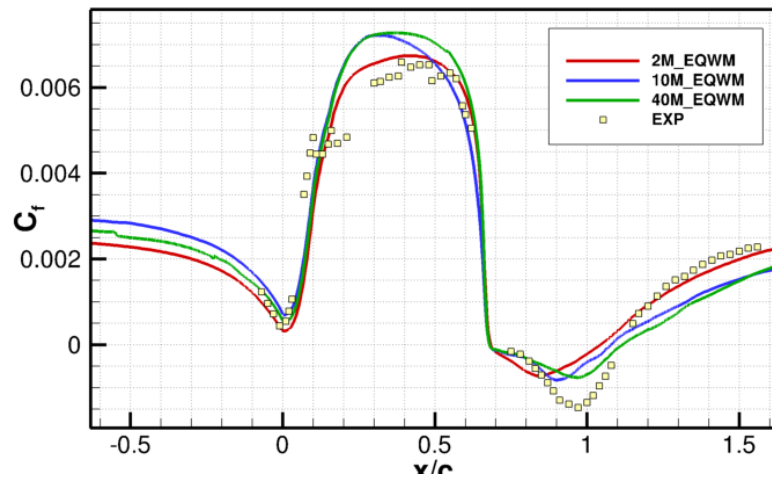
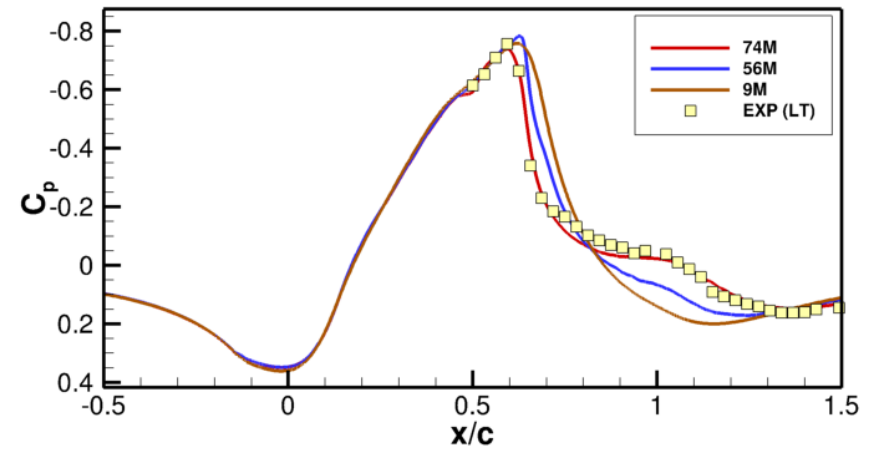
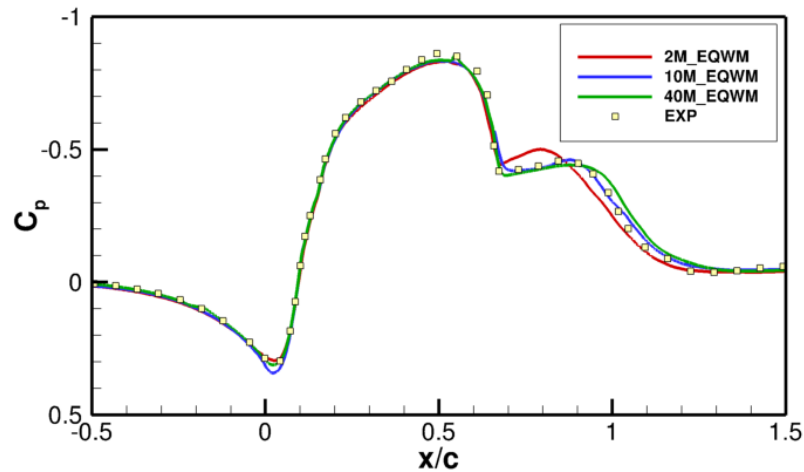
- Good agreement with experiment in the center of the separation bubble for NASA hump case.
- Transonic bump velocity/stress data from smaller tunnel which can explain some discrepancies.
- Separation bubble size within 10% of experiment when computed based on the near-wall velocity vector.

Accelerating Region Comparisons



- Similar velocity predictions for WMLES and RANS.
- WMLES significantly outperforms RANS in predicting turbulent stresses.

Grid Sensitivity for EQWM

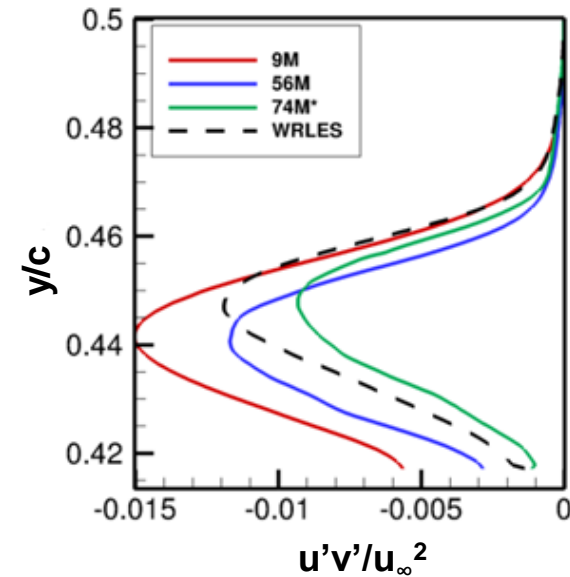
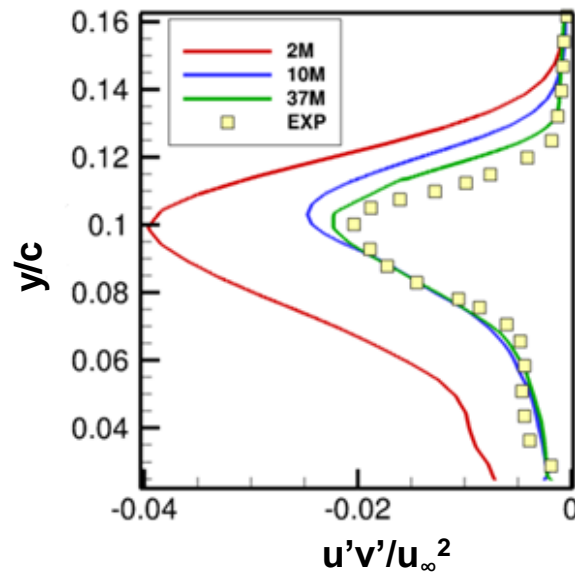
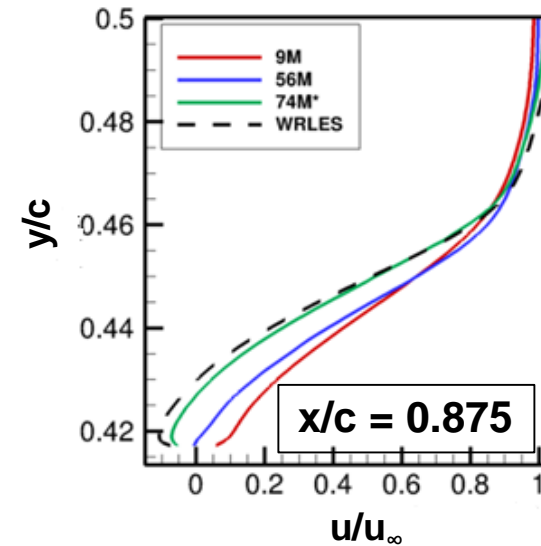
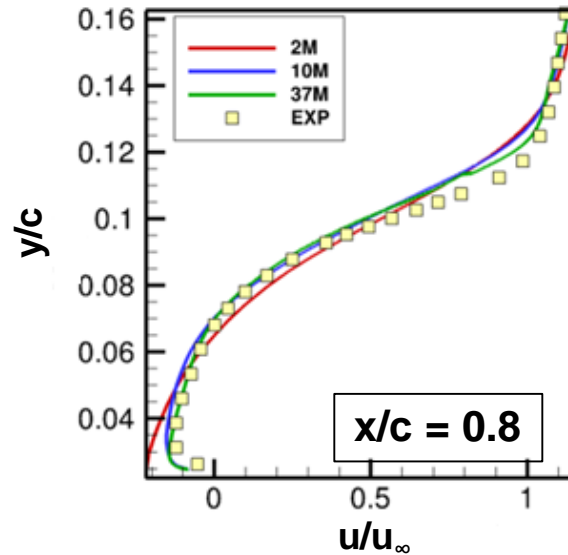


NASA Hump

Transonic Bump

- Improvement in predictions with grid refinement.
- Further refinement would take us close to a WRLES!

Grid Sensitivity for EQWM

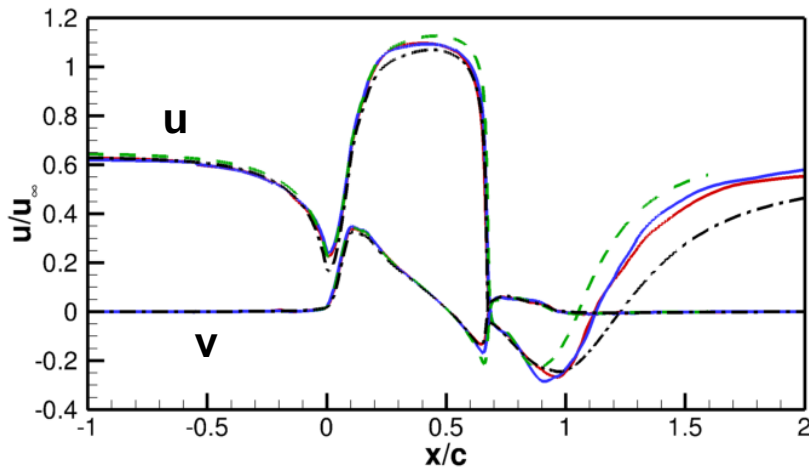
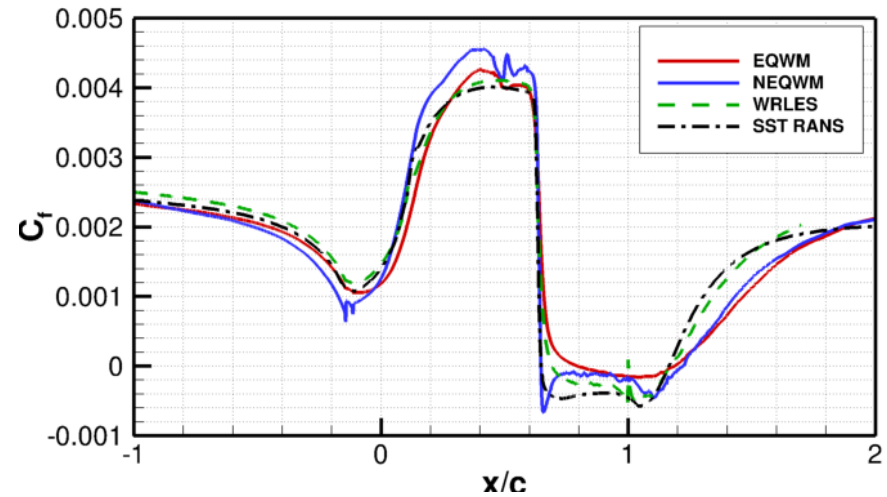
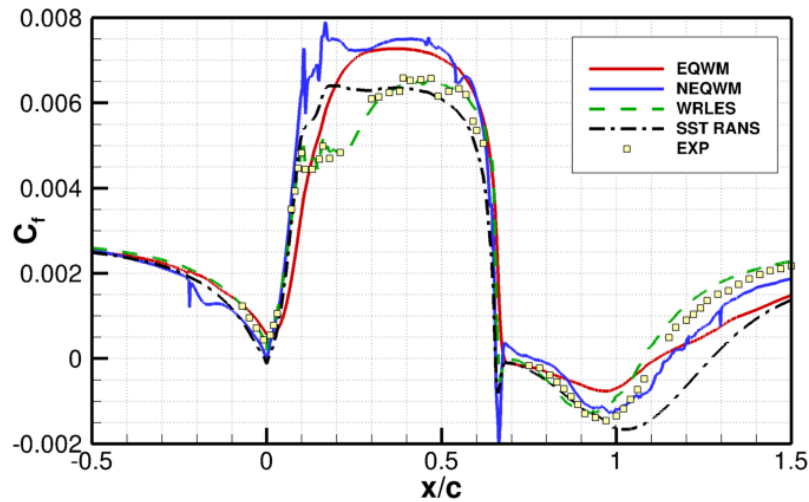


NASA Hump

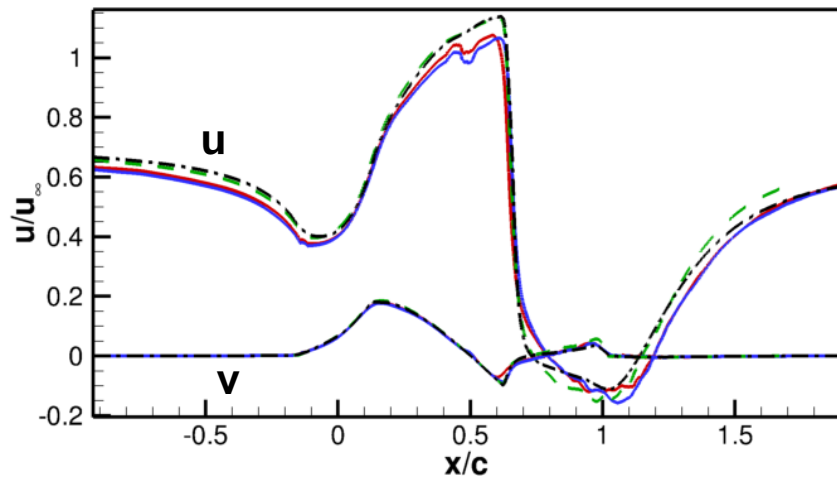
Transonic Bump

- Improvement in predictions with grid refinement. It appears that separation bubble predictions are less dependent on the WM, and more on the LES grid resolution.

EQWM vs. NEQWM at Exchange Location



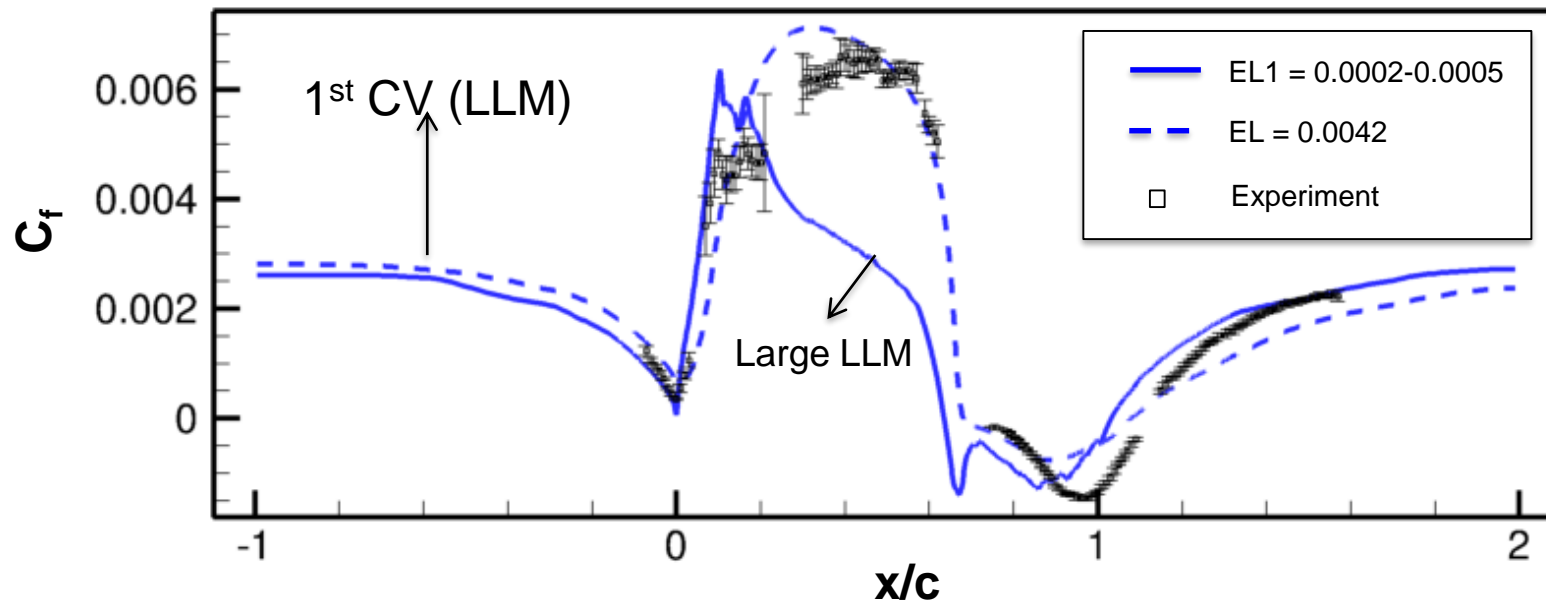
NASA Hump Fine Grid



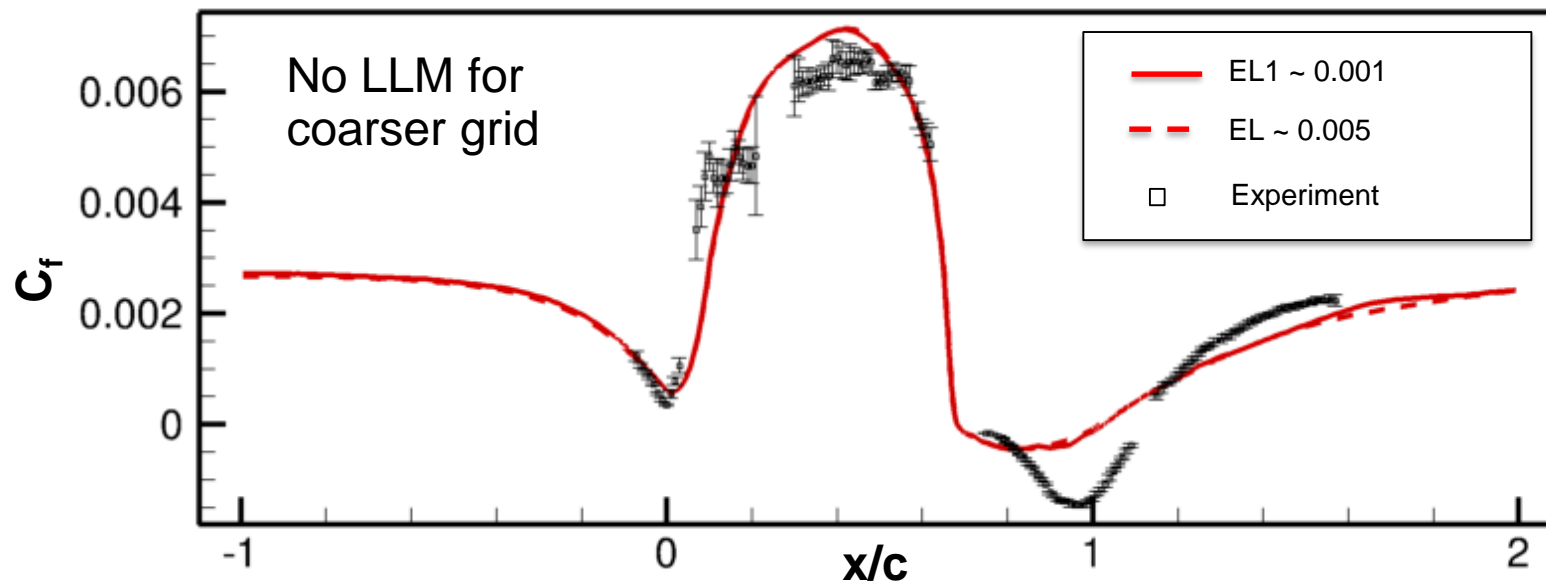
Transonic Bump Fine Grid

- Significant qualitative differences between EQWM and NEQWM C_f .
- But nearly identical time-averaged velocity at the EL!

Exchange Location/ Grid effects for EQWM¹



1st point v/s
> 3rd point EL
for 10M grid

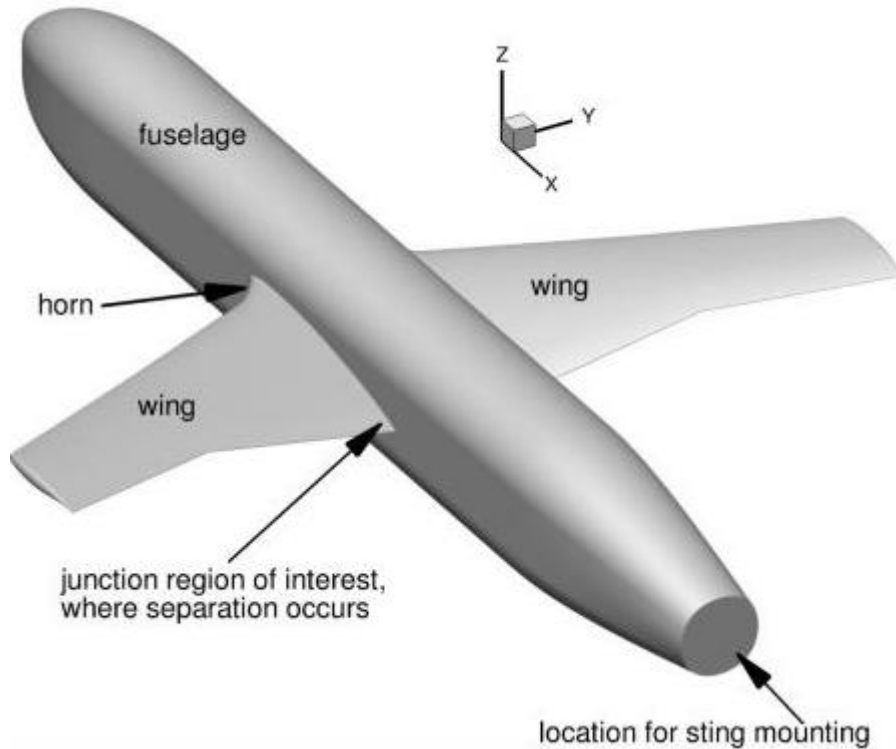


1st point v/s
> 3rd point EL
for 4.4M grid

- Reasonable predictions when using exchange location away > 3rd point.

Juncture Flow Results

Juncture Flow Experiment Details



Fuselage length = 4839.233 mm

Wing-span = 3397.25 mm

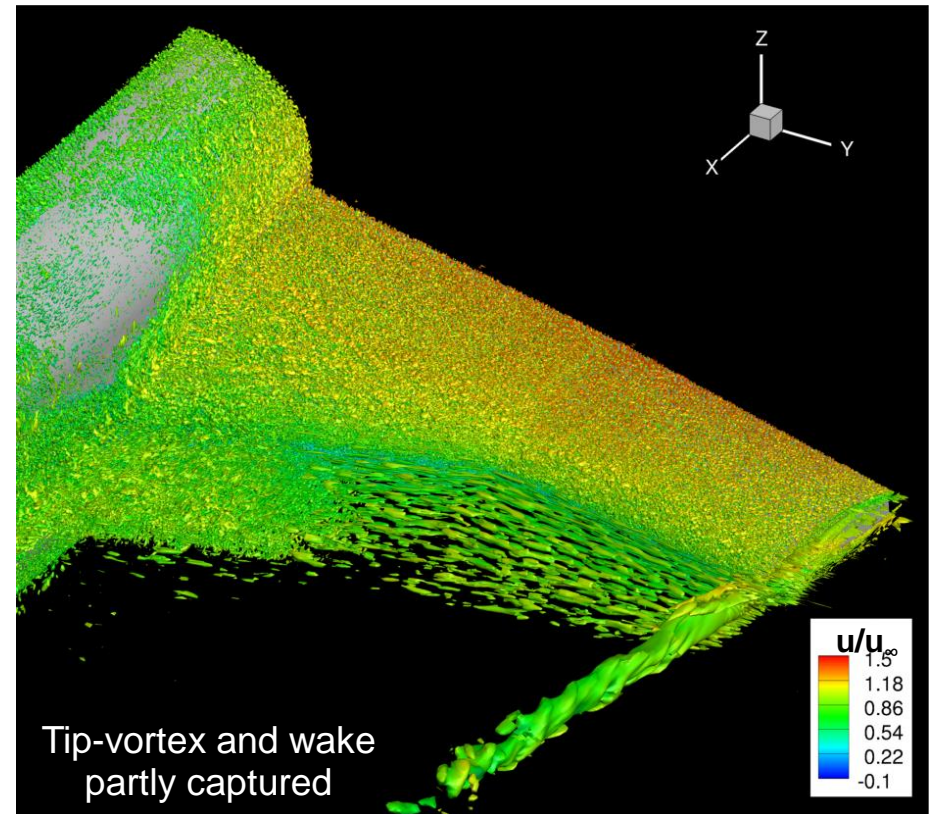
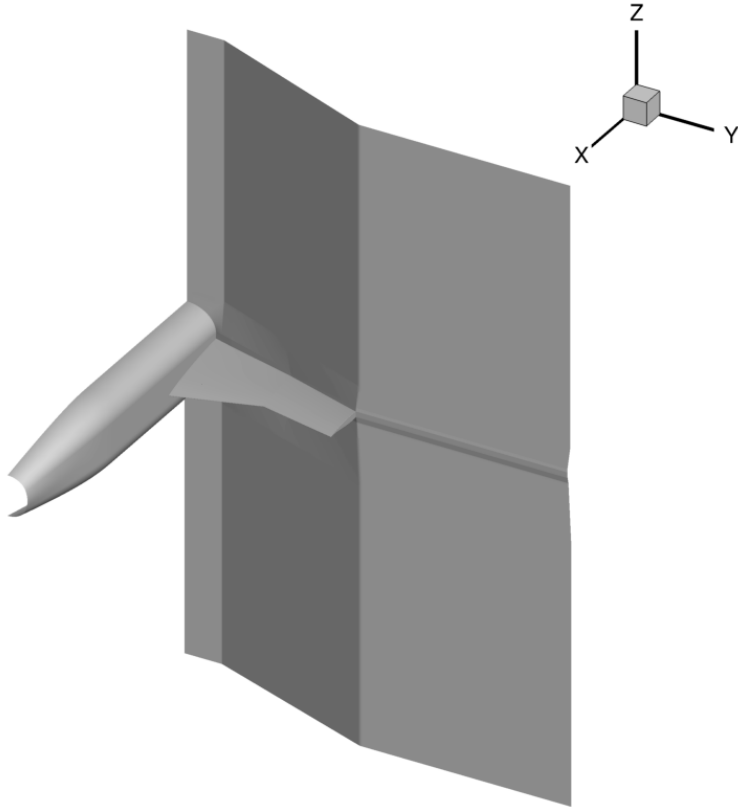
Separation bubble: $x \sim 2840 - 2960$ mm or 118 mm

(for $\alpha = 5^\circ$) $|y| \sim 236 - 278$ mm or 42 mm

M_∞	C	u_∞	T_∞	Re_c	α
0.189	557.17 mm	64.36 m/s	288.84 K	2.4×10^6	5°

- Experiment by Kegerise & Neuhart (2019), F6-based configuration with horn.
- Tunnel Wall, Sting and Mast **neglected** in simulations.
- Attached fuselage and wing BL: $\delta \sim 16$ -20 mm. $Re_\tau \sim 3300$, $\Delta = 1$ mm $\Rightarrow \Delta^+ = 170$.
- Two strategies employed: **Truncated-** and Full-domain Simulations.

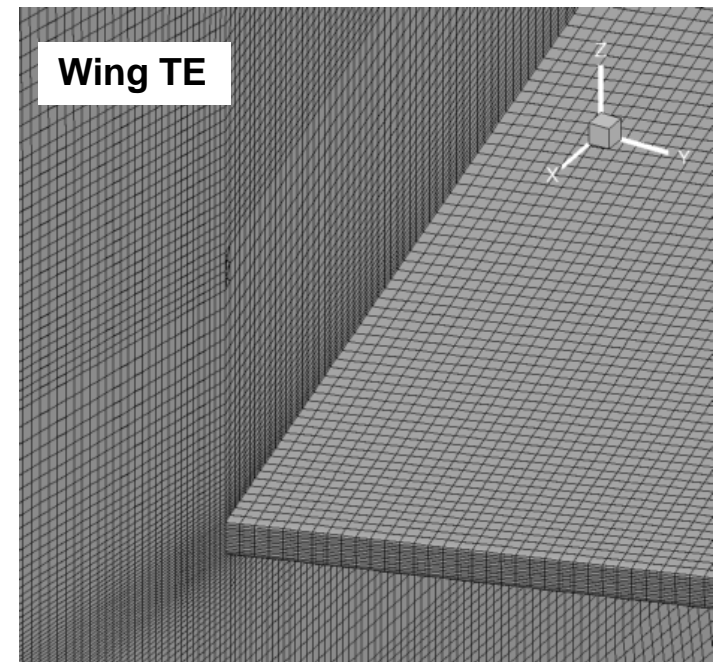
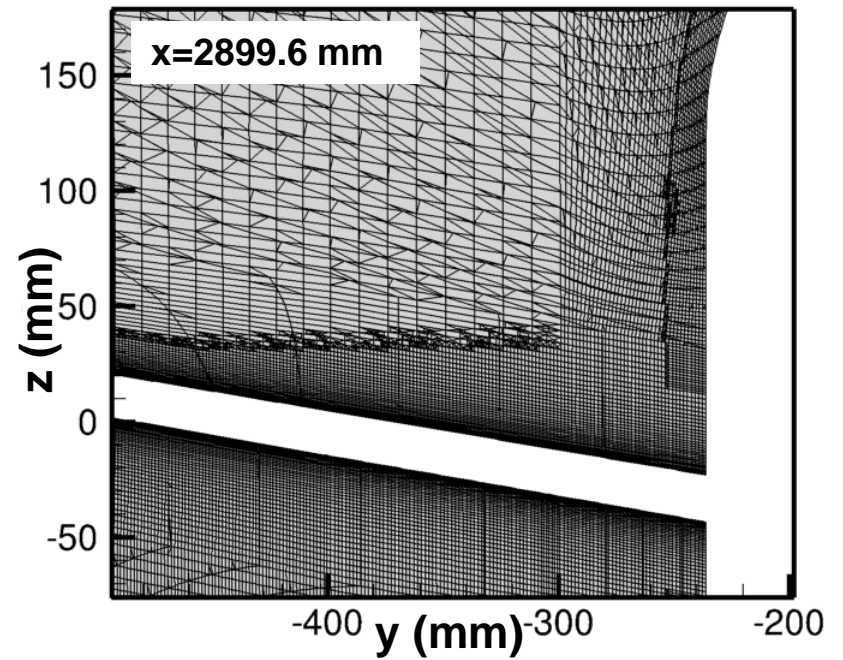
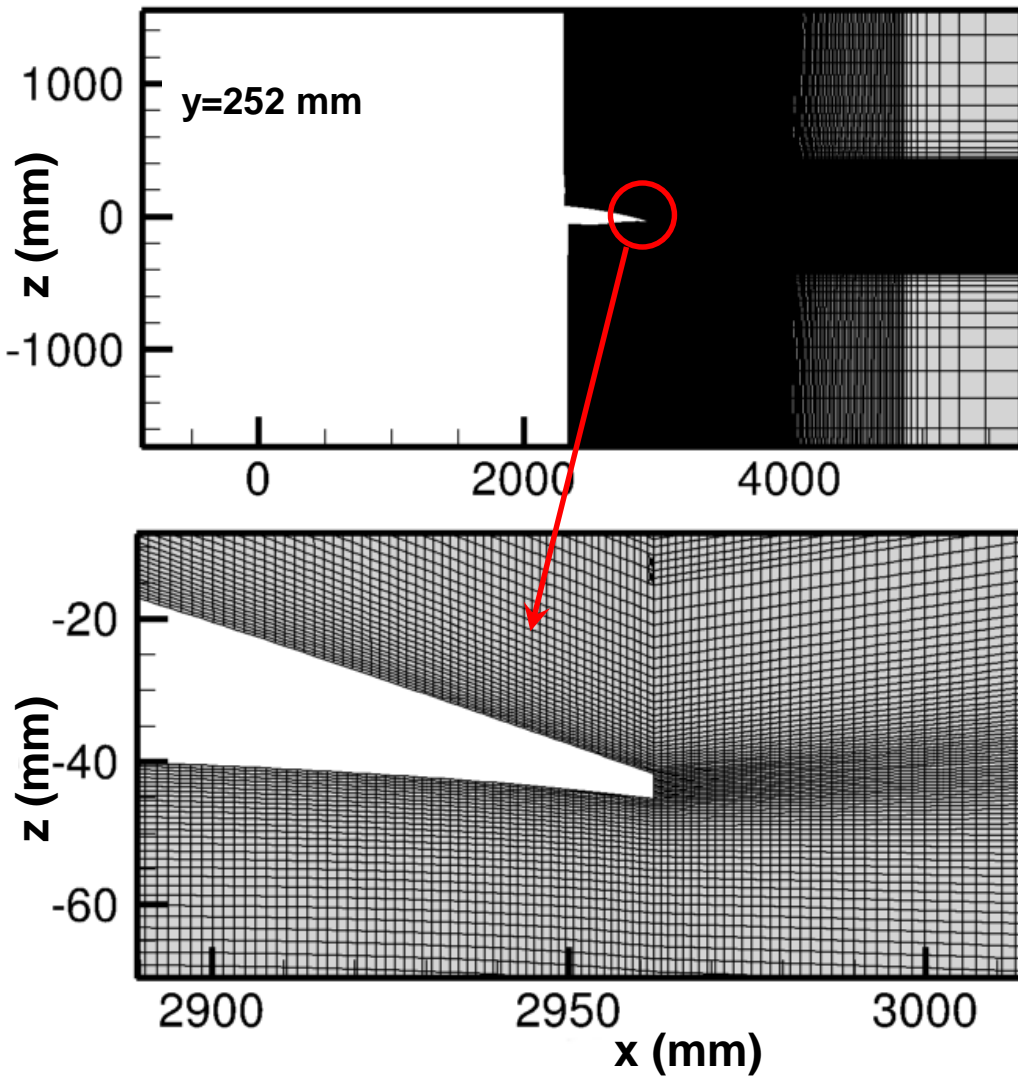
Truncated-Domain Simulation Description



- Only half the geometry simulated ($y=0$ is the symmetry plane). Inflow at $\sim 0.2 - 0.3c$ of the wing such that flow is fully turbulent based on RANS C_f . **Compressible** Solver.
- Grid size = 62 M, with 8 ppd or 2 mm (> 300 in viscous units) wall parallel spacing.
- Mean flow from RANS + synthetic fluctuations using the method of Shur et al. (2014).
- Truncated and Full-domain results reported in [Iyer & Malik, AIAA-2020-1307](#).

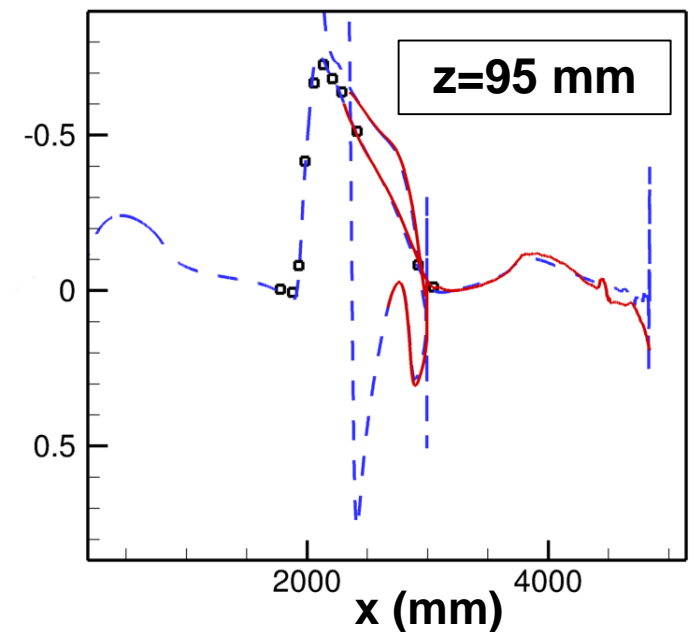
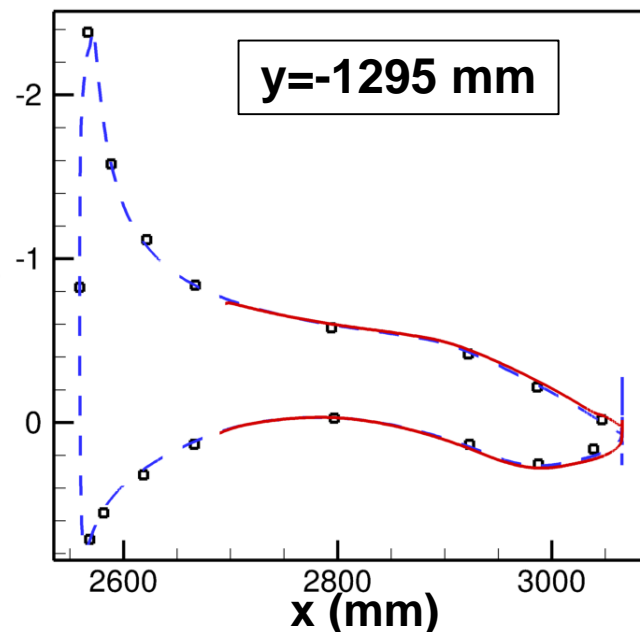
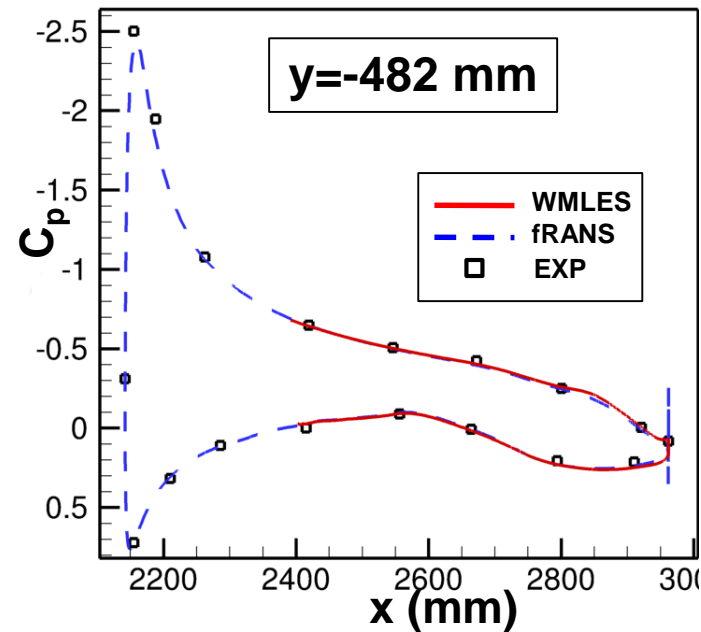
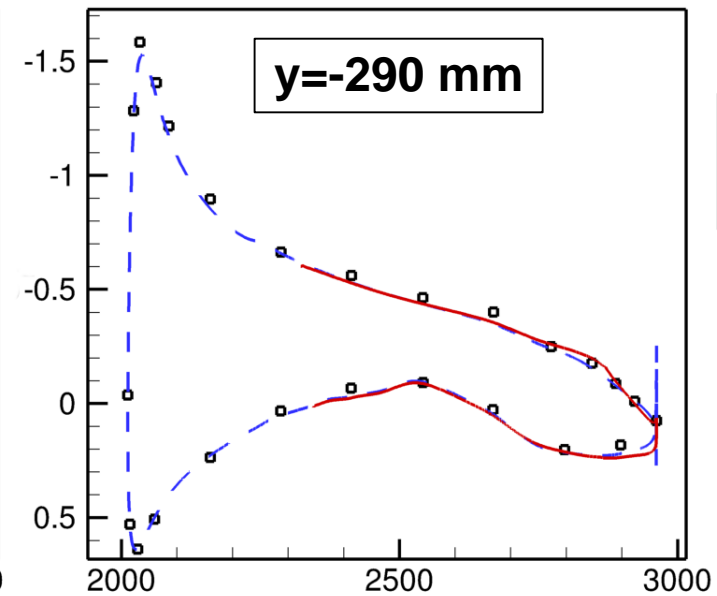
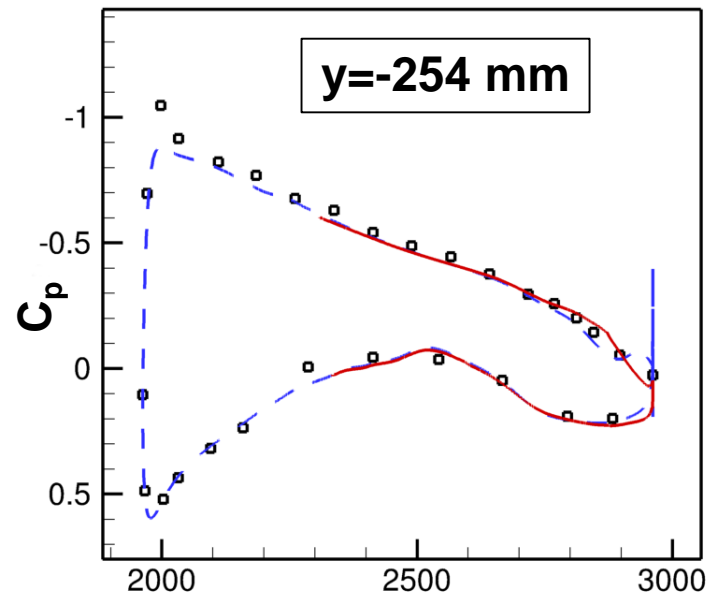
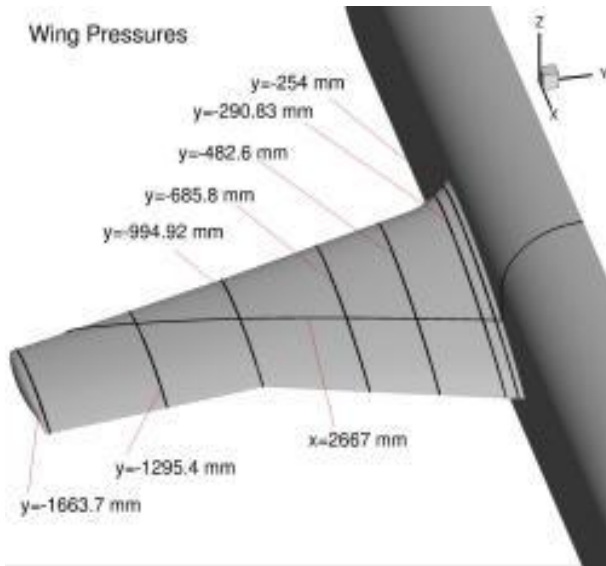
Grid Details

Truncated-Domain (62M)



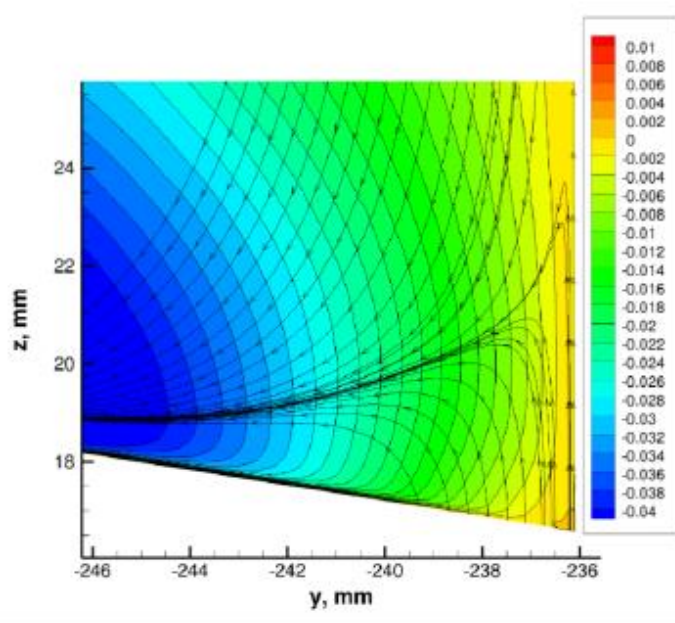
- C-type grid, block-structured grid + near-surface adaptation using *adapt* tool in Charles.
- 16 points in wall-normal direction per δ with minimum near-wall spacing of 0.3 – 1 mm or ($\Delta n^+ \sim 60$ -170).

Wall Pressure Comparisons

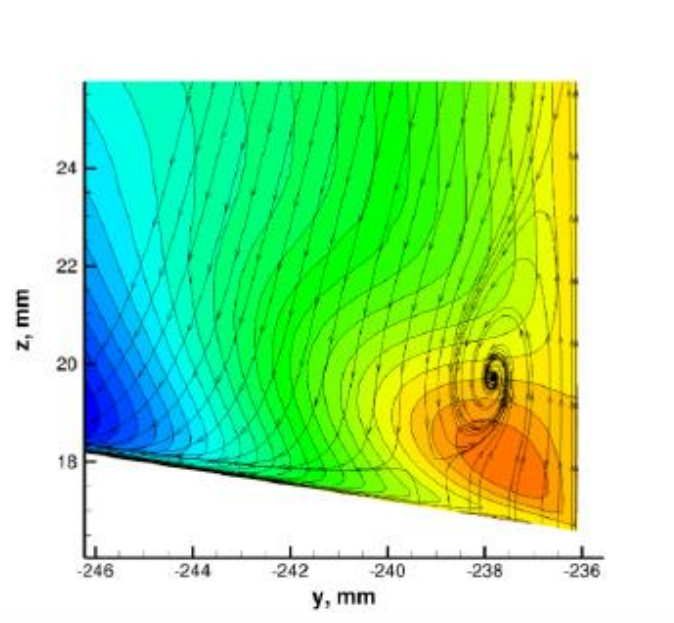


- Good agreement except at wing trailing edge at $y = -254$ mm.
- Fine Grid SA-RC-QCR2013 RANS from Rumsey et al. (2019).

Corner Vortex at x=2747.6 mm



(c) Contours of v/U_{ref} from FUN3D with in-plane streamtraces of $(v, w + 0.11)$, SA-RC model, F grid



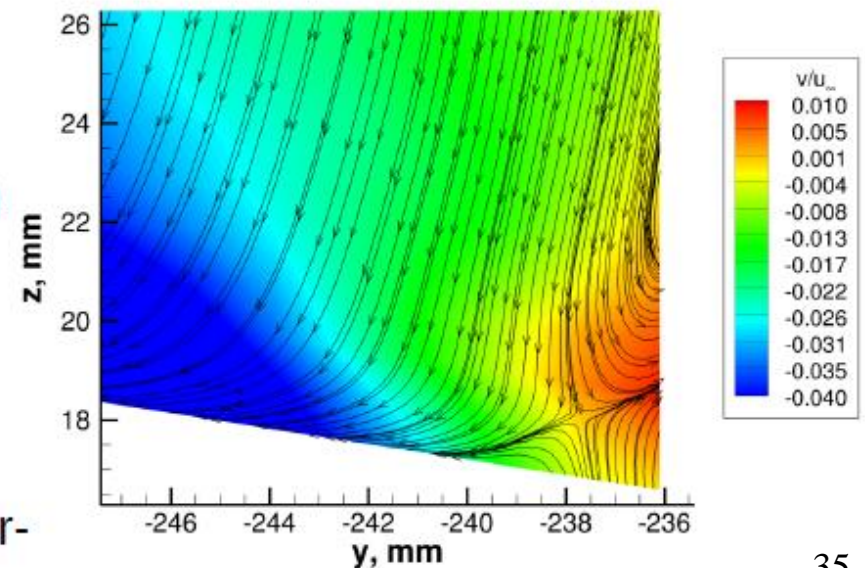
(d) Contours of v/U_{ref} from FUN3D with in-plane streamtraces of $(v, w + 0.11)$, SA-RC-QCR2013-V model, F grid

**FUN3D
RANS**

(Rumsey et al., AIAA-2020-1304)

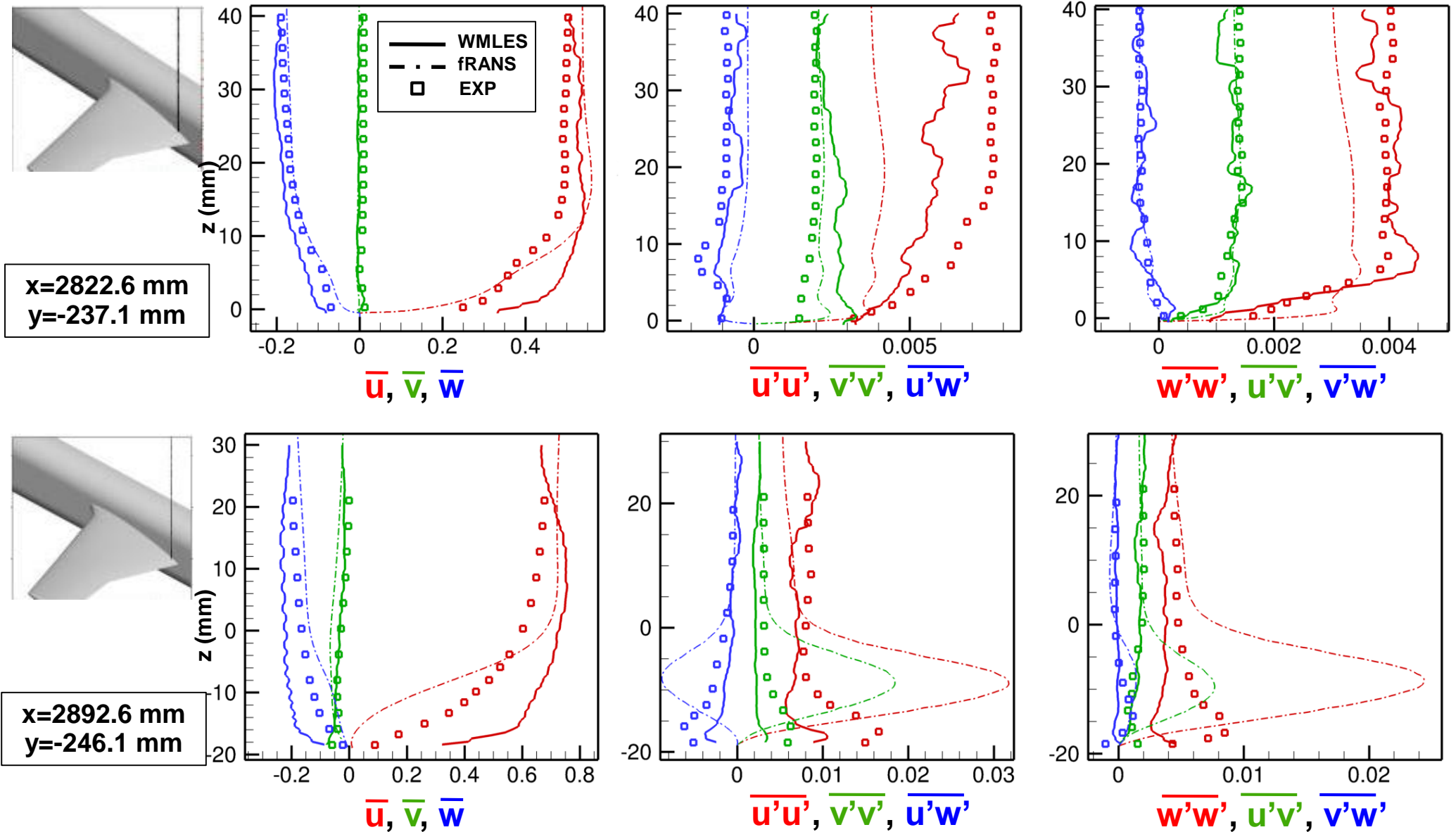
(Experimental separation at $x \sim 2840$ mm)

**WMLES
Truncated domain
62M simulation**



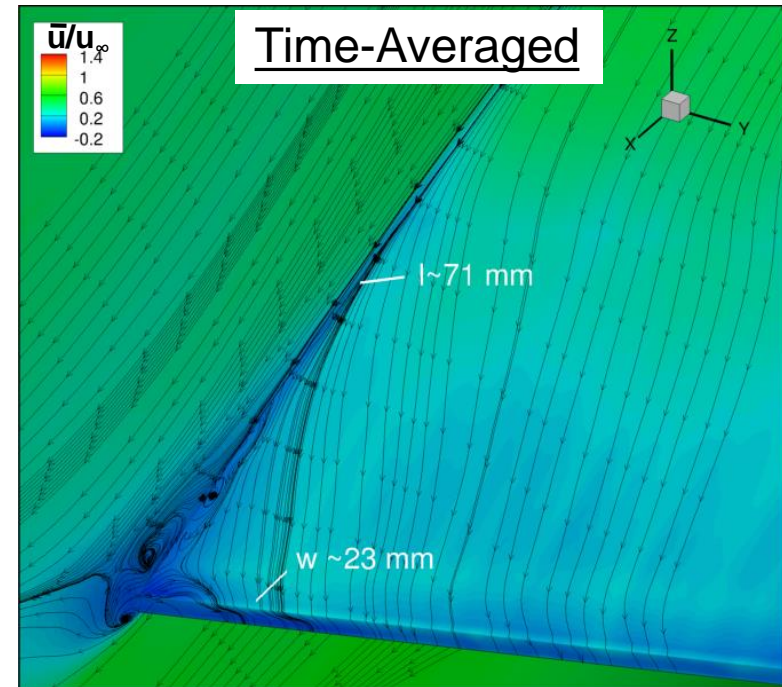
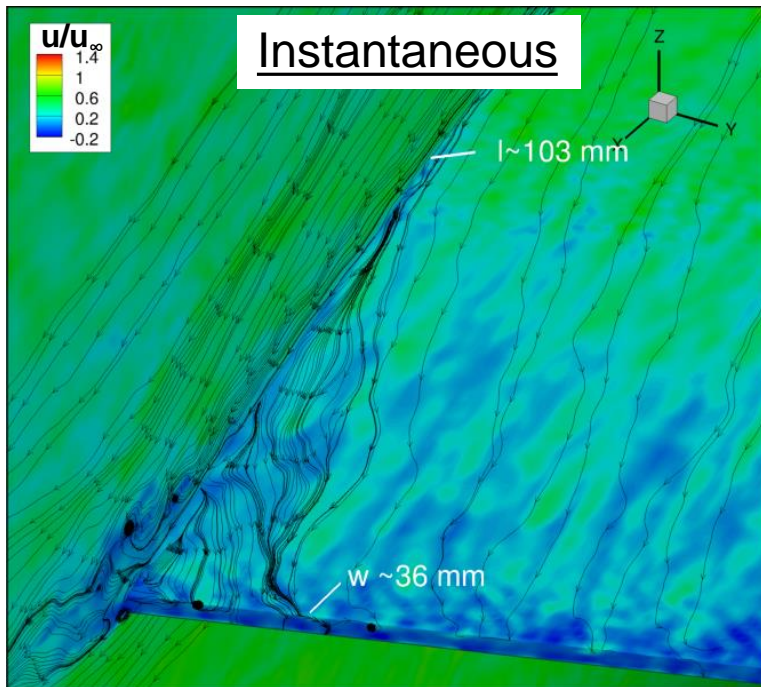
- Corner vortex not observed in WMLES due to near-wall errors and/ or resolution.

Velocity and Stress Comparisons

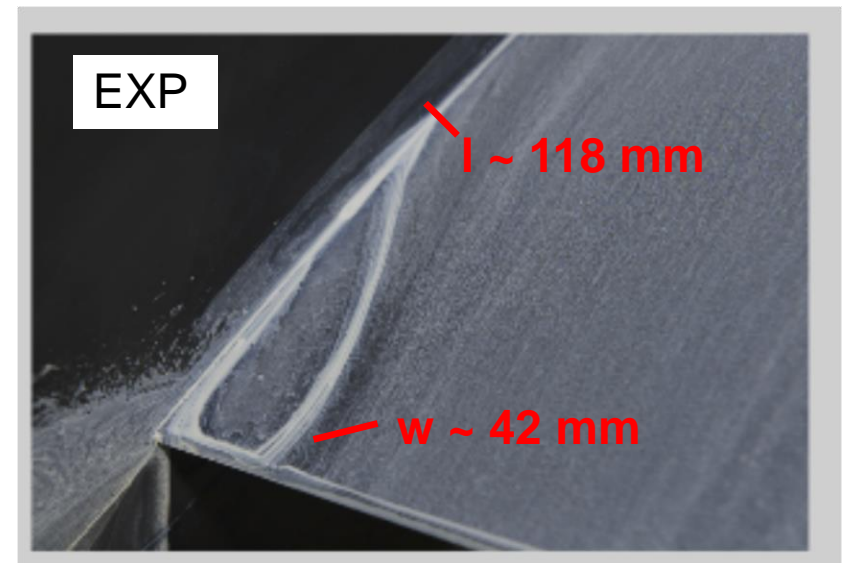


- Reasonable agreement with experiment. Differences due to underprediction of bubble size in WMLES.
- Better prediction of stresses when compared to RANS.

Separation Bubble Comparisons

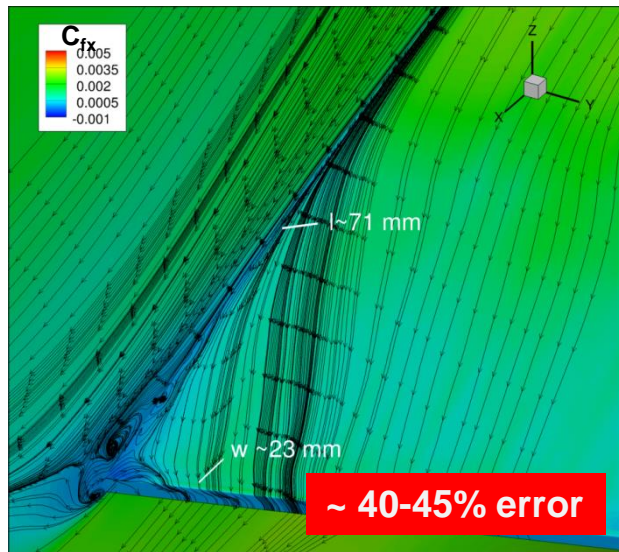


- Bubble size underpredicted by WMLES by ~40-45% in the mean.
- Instantaneous bubble larger, and closer to the experimental value by ~20%.
- However, the near-wall streamlines are inaccurate which could be due to the deficiencies of the EQM model used here.



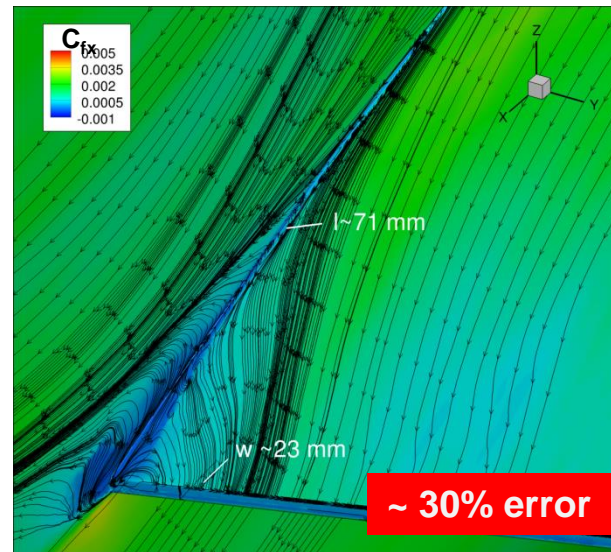
WMLES Bubble Predictions

62M-TD

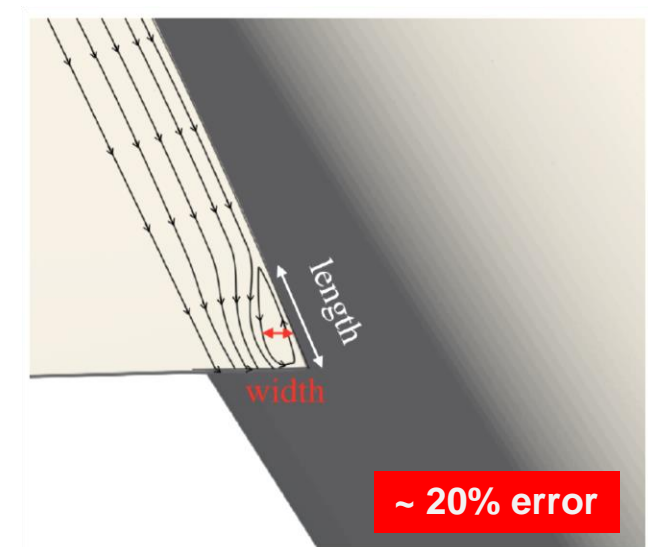


Iyer & Malik (AIAA-2020-1307)
CharLES Unstructured

90M-FD

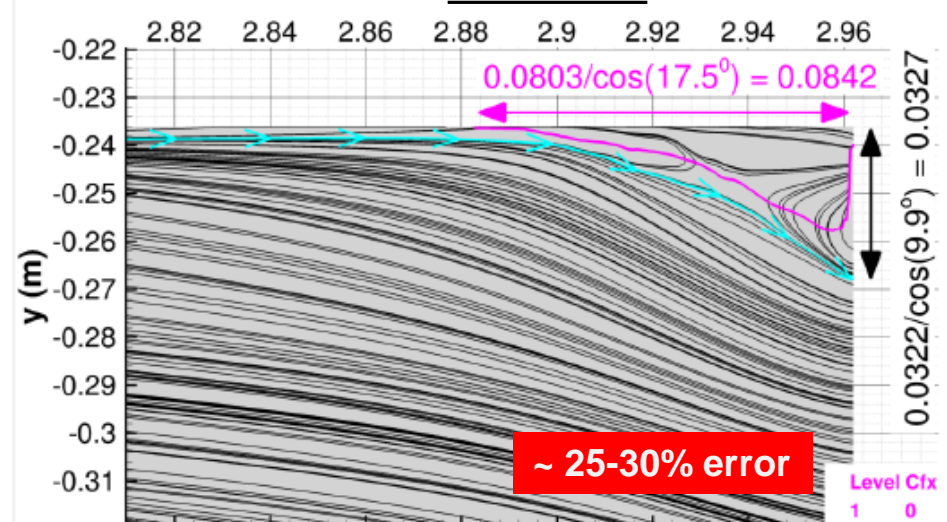


122M-FD

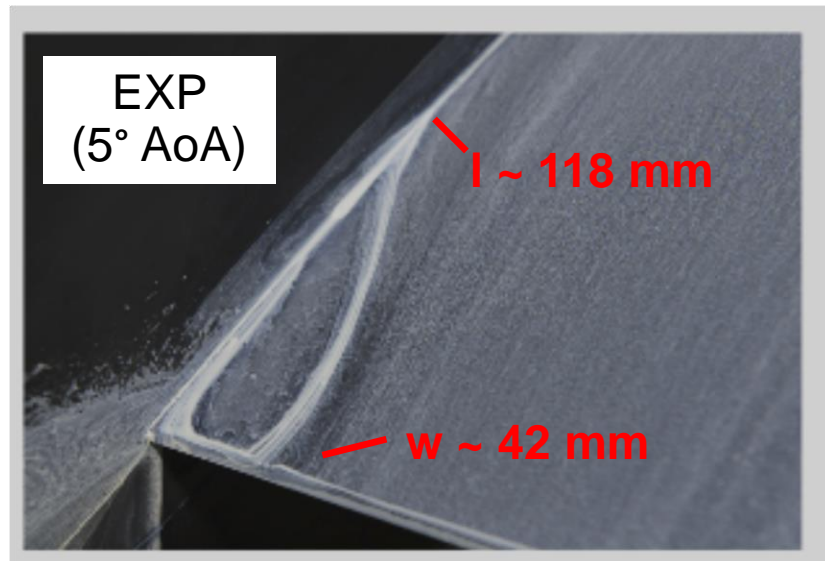


Lozano-Duran et al. (AIAA-2020-1776)
CharLES Voronoi

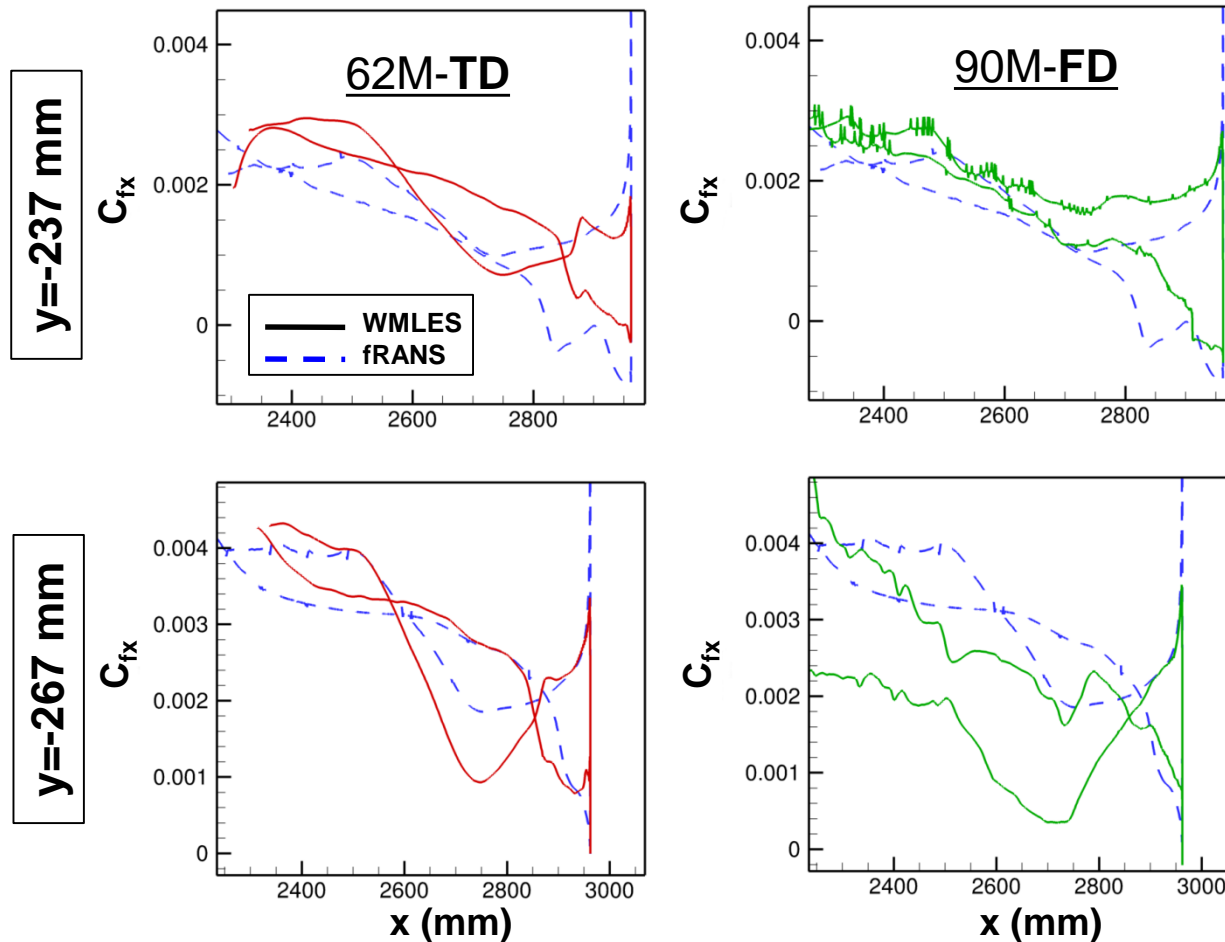
440M-FD



Ghate et al. (AIAA-2020-2735)
LAVA Structured-Overset



Full- and Truncated-Domain Comparisons



- Slight overprediction in C_f at $y = -237$ mm [EQWM effect on corner flows] likely causing delayed separation.
- Away from the corner, tripping appears to be less effective on the lower surface of the wing with favorable pressure gradient, while the synthetic inflow turbulence yields better predictions on both top and bottom surfaces.

Summary

- Sources of error/ uncertainty in WMLES predictions

- A number of them discussed, some of which have fixes like LLM
- Some important outstanding ones :
 - Wall-stress Fluctuations
 - Pressure Gradient/ Acceleration effects on Eddy Viscosity
 - Accuracy of LES SGS model for more complex situations, and varying grid anisotropies
 - Bubble size incorrectly predicted by C_f if $EL > 1^{\text{st}}$ grid point
- Similar issues exist in DES-based approaches as well

- Suggested Grid Design

- $EL \sim 5\%$ of δ , and $EL > 1$ -2 wall parallel spacing (Kawai & Larsson 2012)
- Near-isotropic aspect ratios except very near wall
- Coarse 8-16 ppd resolution appears to be sufficient for attached regions
- Need to add refinement in acceleration, shock, pressure gradient regions to accurately capture physical features such as bubble, shear layer, secondary BL etc.
- Difficult to estimate requirements *a priori*. Grid adaptation would greatly help!
- DNS and WMLES require same grid resolution to capture shock, and so WMLES not cheaper in such regions.

- RCA Test Cases

- Good agreement with experiment/ WRLES data for finest grid.
- Results improve with grid refinement
- Improved prediction of turbulent stresses in accelerating and separation regions when compared to RANS.

- Juncture Flow

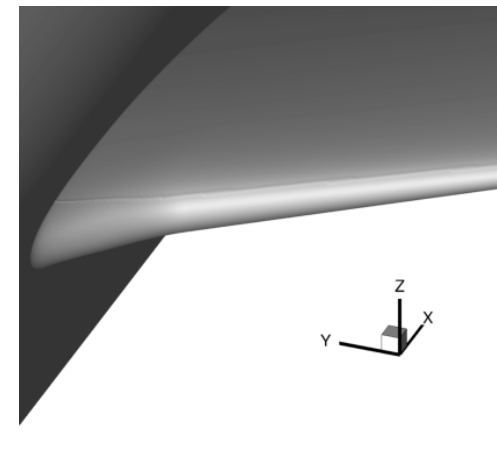
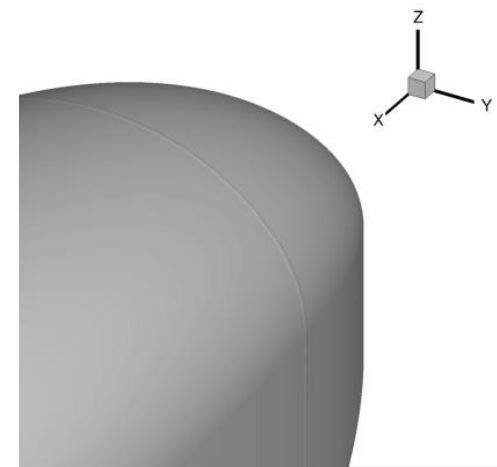
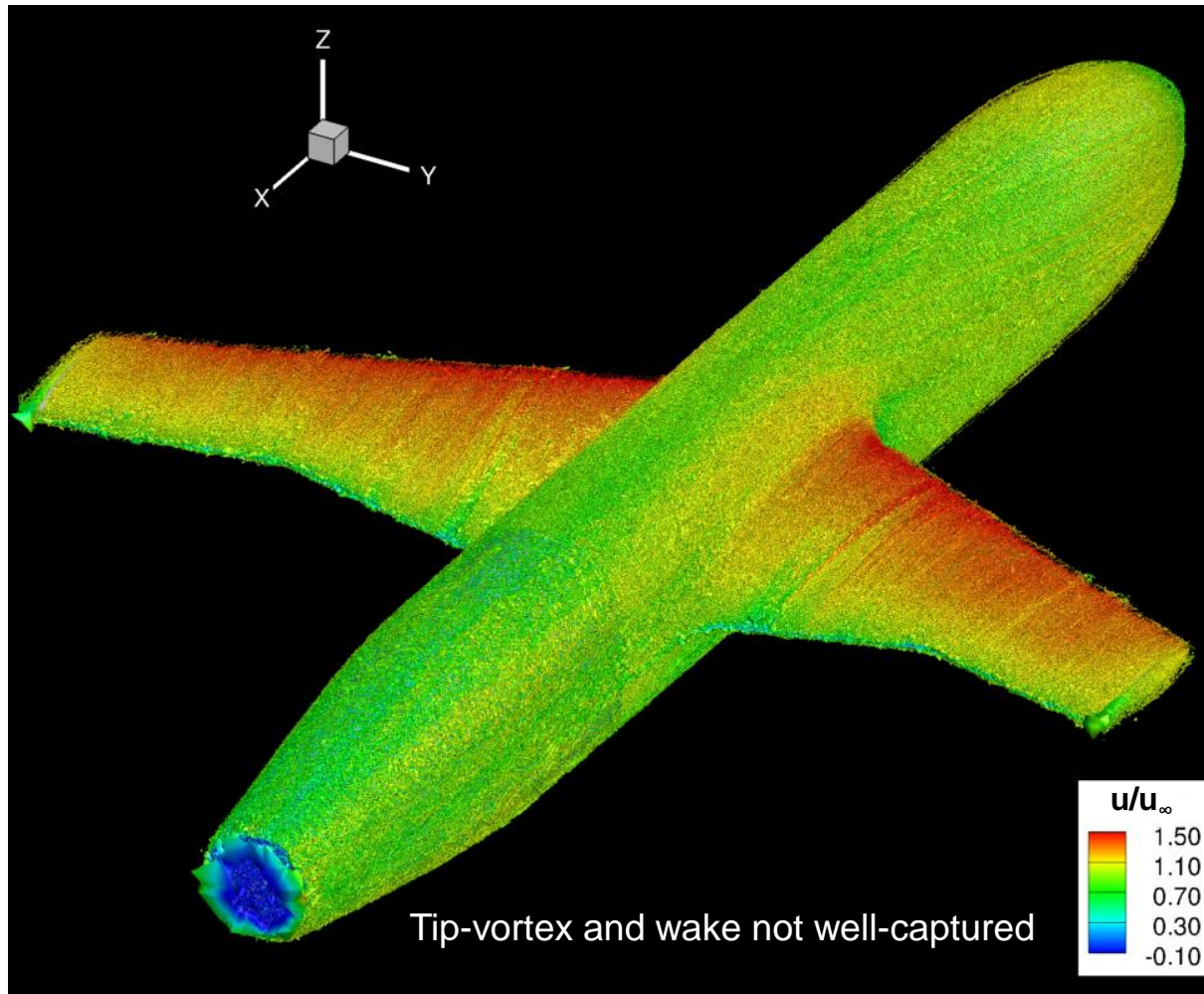
- Overprediction of C_f in corner regions causing smaller bubble.
- Preliminary coarse grid results encouraging, but need significantly finer grid (0.5-1B) to accurately predict stresses in the separation region.

Acknowledgements

- Support from NASA Transformational Tools and Technologies (TTT) Project
- Cascade Technologies for providing the *CharLES* solver and support.
- Prof. George Park for help with nonequilibrium model version of code.
- Langley K-cluster and NAS HEC Program for compute resources.
- Dr. Ali Uzun and Dr. Chris Rumsey for useful discussions and data.

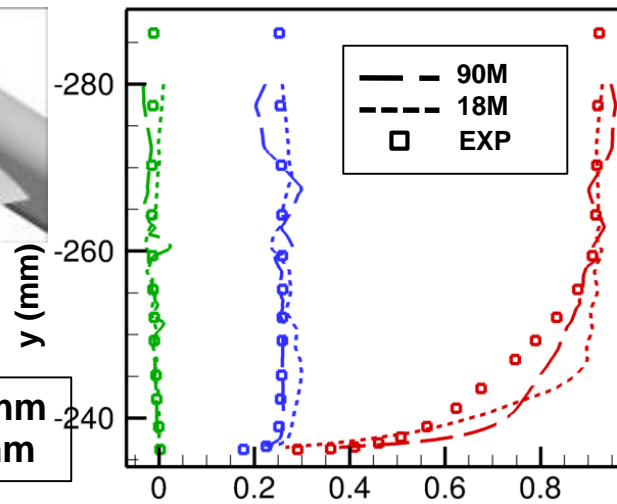
Backup Slides for JF

Full-Domain Simulation Description

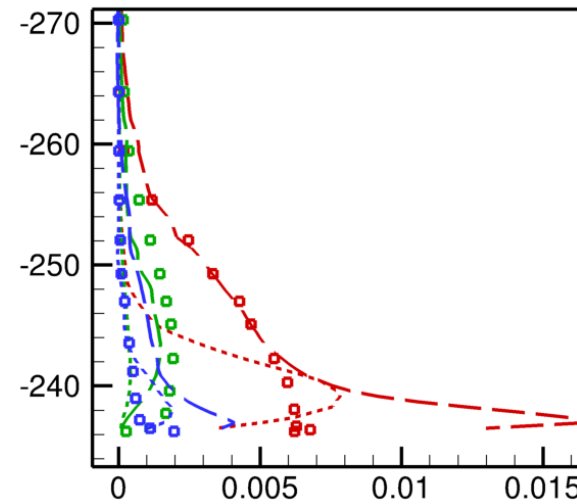


- Full geometry with 2D trips (cylindrical dots in experiment) to trigger turbulence. **Incompressible** solver, implicit CFL=5.
- Grid size = 18 and 90M, with 4 and 8 ppd wall parallel spacing ($\delta \sim 16\text{-}20$ mm).
- Surface points displaced at trip locations (by 80% of first wall-normal spacing) matched with experiment, but trip height is 0.8 and 0.4 mm for the coarse and fine grids, while the experimental height varies between 0.17 and 0.29 mm with a diameter of 1 mm.

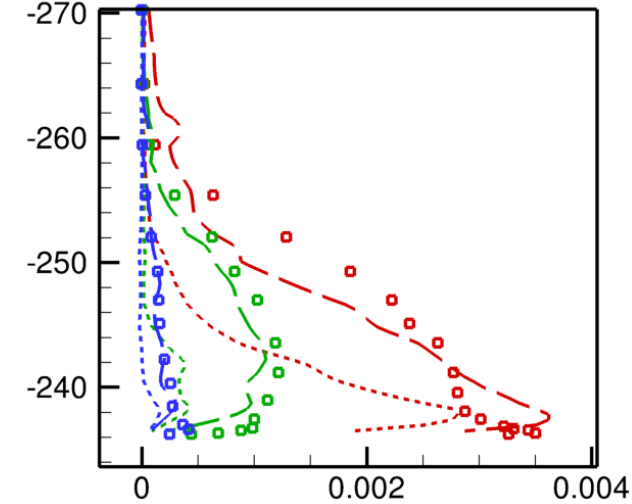
FD JF Velocity and Stress Comparisons



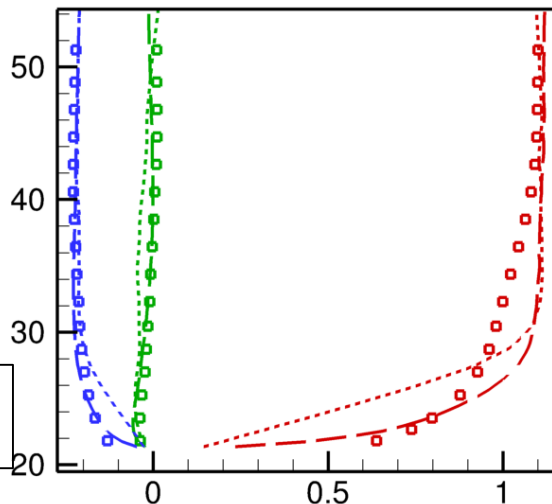
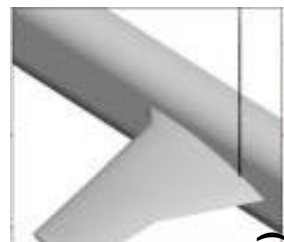
\bar{u} , \bar{v} , \bar{w}



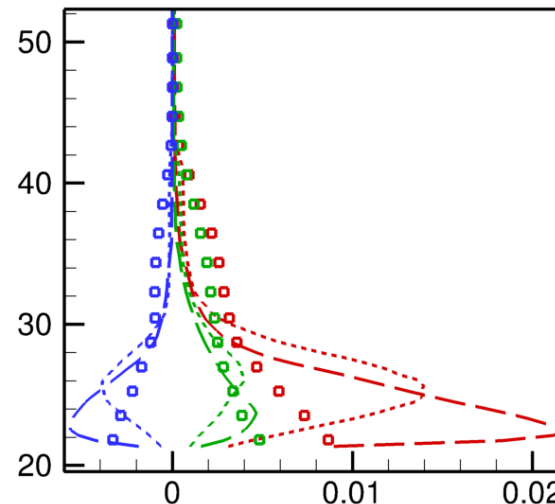
$\overline{u'u'}$, $\overline{v'v'}$, $\overline{u'w'}$



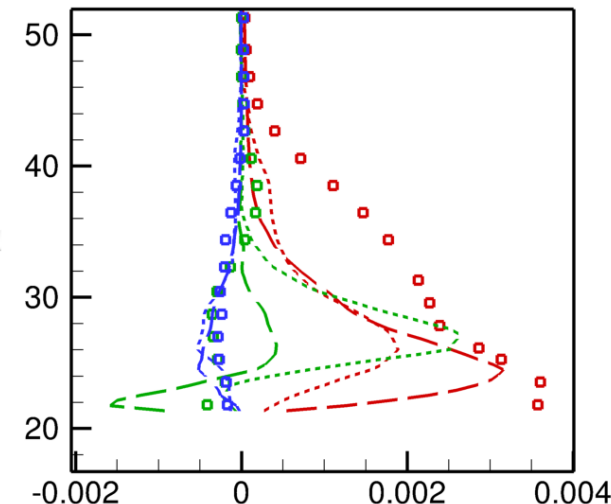
$\overline{w'w'}$, $\overline{u'v'}$, $\overline{v'w'}$



\bar{u} , \bar{v} , \bar{w}



$\overline{u'u'}$, $\overline{v'v'}$, $\overline{u'w'}$

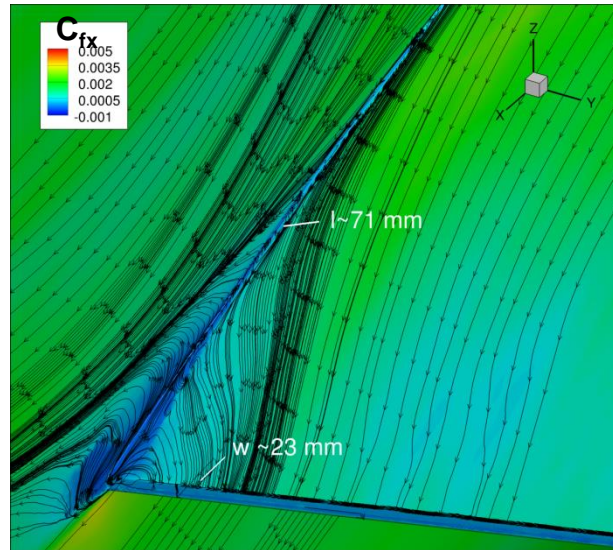


$\overline{w'w'}$, $\overline{u'v'}$, $\overline{v'w'}$

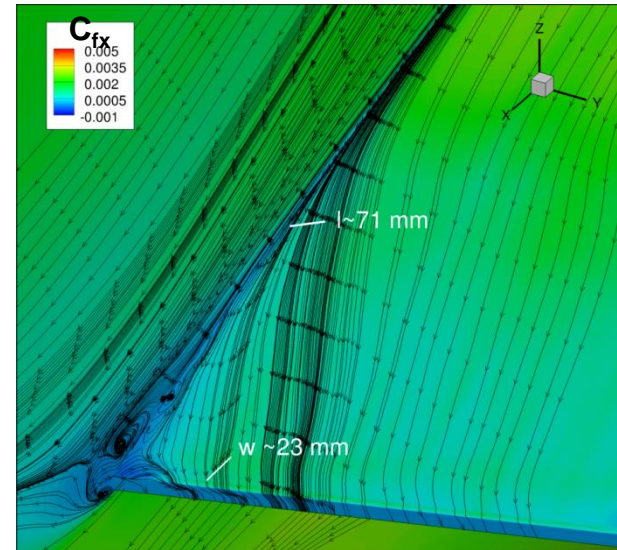
- Further improvement in u velocity and $u'u'$ needed.
- 8 ppd gives superior predictions compared to the 4 ppd grid.
- $u'u'$ overpredicted near the wall. Tripping strategy likely needs improvement.

Full- and Truncated-Domain Comparisons

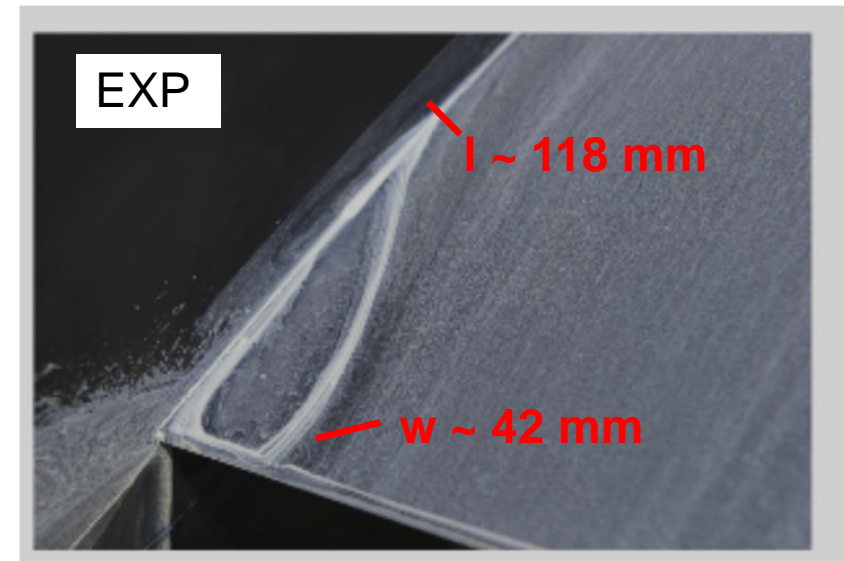
90M-FD



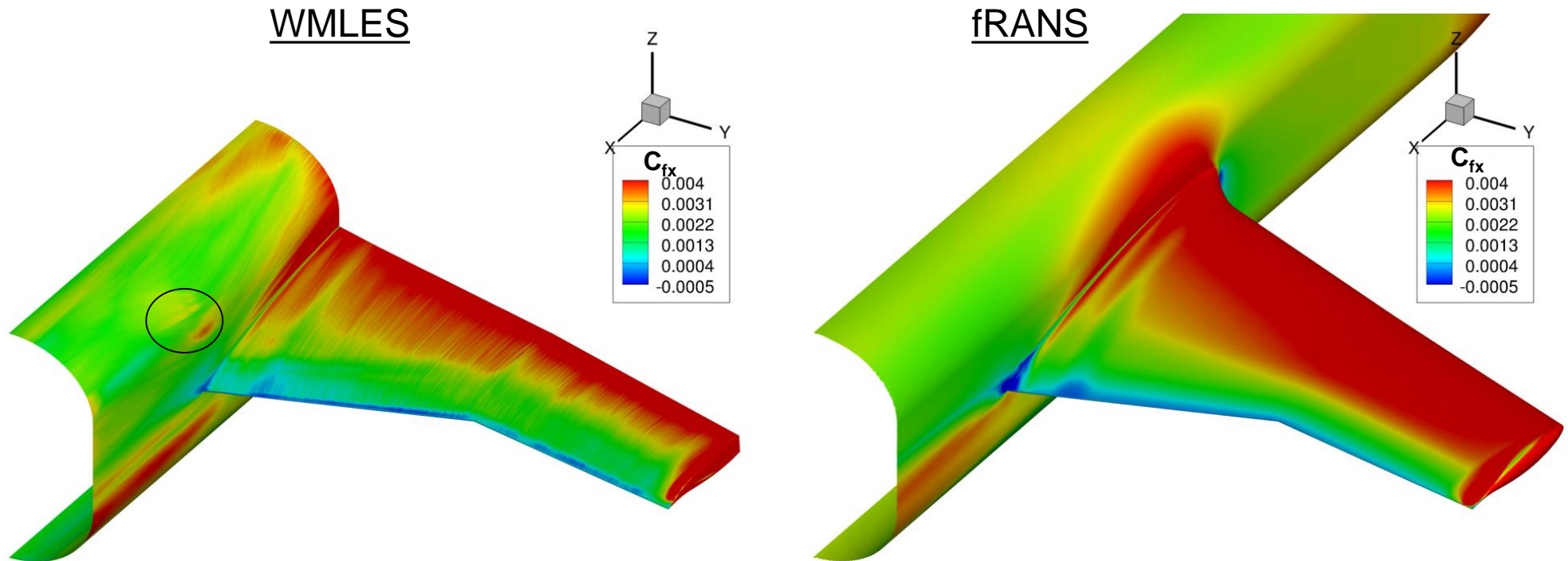
62M-TD



- 8 ppd full- and truncated-domain simulations predict similar bubble size and shape.
- Bubble size underpredicted by WMLES by ~40-45% in the mean for the 8 ppd grids.

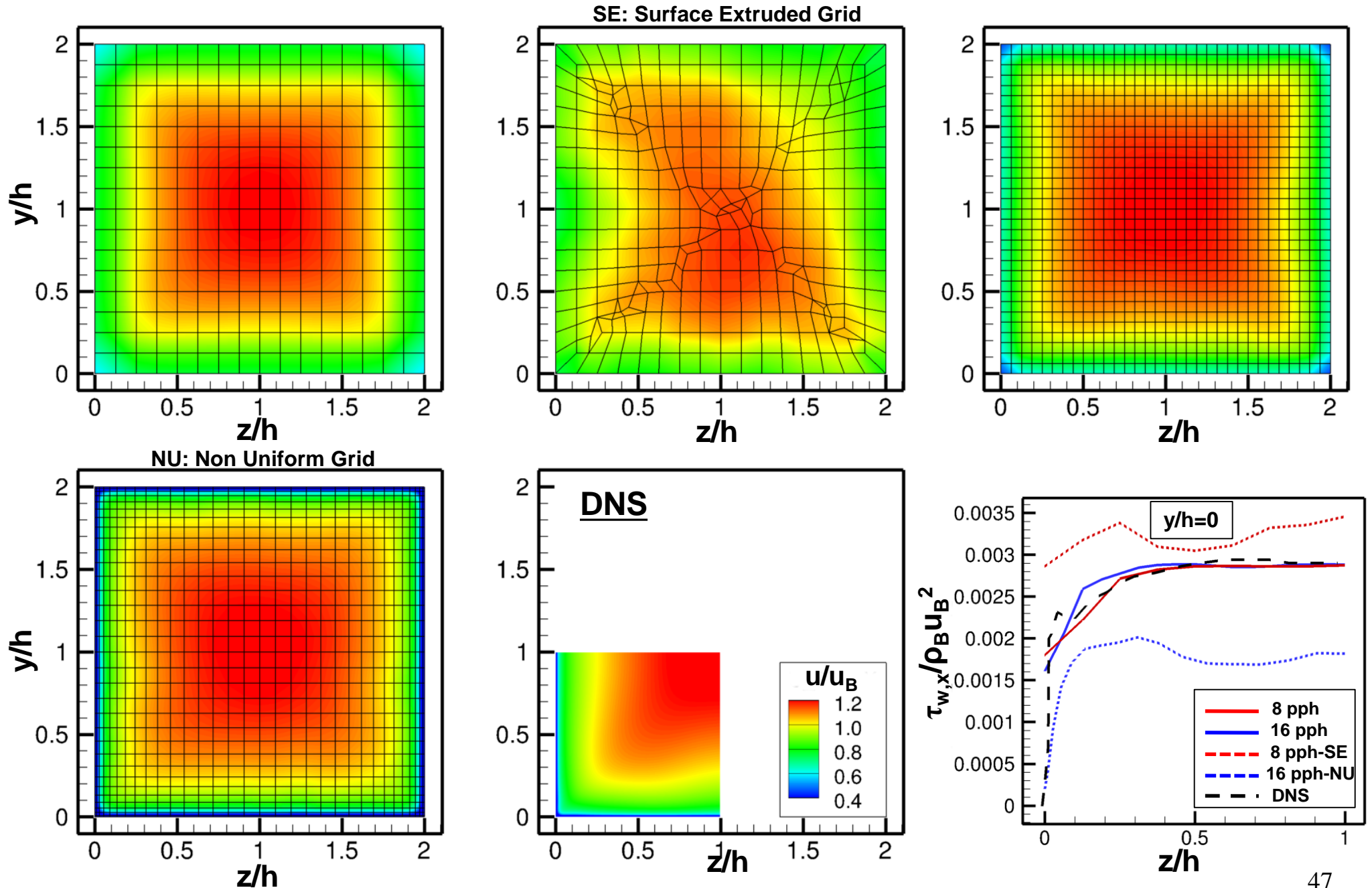


Wall Skin-friction Comparisons



- Fairly good agreement with fine grid SA-RC-QCR2013 RANS from Rumsey et al. (2019) indicating the effectiveness of synthetic inflow turbulence.
- Minor anomaly above trailing edge on fuselage , could be grid/ adaptation related.

Turbulent Square Duct Results



- Uniform, structured grids yield better predictions, but still overpredicts C_f near corner.